in human multidrug-resistant leukemia cells. *Blood.* 1992;79(12):3267-3273.

31. Carella AM, Berman E, Maraone MP, Ganzina F. Idarubicin in the treatment of acute leukemias: an overview of preclinical and clinical studies. *Haematologica.* 1990;75(2):159-169.
32. Kuffel MJ, Ames MM. Comparative resistance of idarubicin, doxorubicin and their C-13 alcohol metabolites in human MDR1 transfected NIH-3T3 cells. *Cancer Chemother Pharmacol.* 1995;36(3): 223-226.
33. Hollingshead LM, Faulds D. Idarubicin: a review of its pharmacodynamic and pharmacokinetic properties, and therapeutic potential in the chemotherapy of cancer. *Drugs.* 1991;42(4): 690-719.
34. Creutzig U, Ritter J, Zimmermann M, et al. Idarubicin improves blast cell clearance during induction therapy in children with AML: results of study AML-BFM 93. *Leukemia.* 2001;15(3):348-354.
35. Cassileth PA, Lynch E, Hines JD, et al. Varying intensity of postremission therapy in acute myeloid leukemia. *Blood.* 1992;79(8):1924-1930.
36. Cassileth PA, Harrington DP, Appelbaum FR, et al. Chemotherapy compared with autologous or allogeneic bone marrow transplantation in the management of acute myeloid leukemia in first remission. *N Engl J Med.* 1998;339(23): 1649-1656.
37. Pautas C, Merabet F, Thomas X, et al. Randomized study of intensified anthracycline doses for induction and recombinant interleukin-2 for maintenance in patients with acute myeloid leukemia age 50 to 70 years: results of the ALFA-9801 Study. *J Clin Oncol.* 2010;28(5): 808-814.
38. Mayer RJ, Davis RB, Schiffer CA, et al. Intensive postremission chemotherapy in adults with acute myeloid leukemia. *N Engl J Med.* 1994;331(14): 896-903.

blood

2011 117: 2366-2372
Prepublished online December 29, 2010;
doi:10.1182/blood-2010-07-295279

A randomized comparison of 4 courses of standard-dose multiagent chemotherapy versus 3 courses of high-dose cytarabine alone in postremission therapy for acute myeloid leukemia in adults: the JALSG AML201 Study

Shuichi Miyawaki, Shigeki Ohtake, Shin Fujisawa, Hitoshi Kiyoi, Katsuji Shinagawa, Noriko Usui, Toru Sakura, Koichi Miyamura, Chiaki Nakaseko, Yasushi Miyazaki, Atsushi Fujieda, Tadashi Nagai, Takahisa Yamane, Masafumi Taniwaki, Masatomo Takahashi, Fumiharu Yagasaki, Yukihiko Kimura, Norio Asou, Hisashi Sakamaki, Hiroshi Handa, Sumihisa Honda, Kazunori Ohnishi, Tomoki Naoe and Ryuzo Ohno

Blood (print ISSN 0006-4971, online ISSN 1528-0020), is published weekly by the American Society of Hematology, 2021 L St, NW, Suite 900, Washington DC 20036.

A randomized comparison of 4 courses of standard-dose multiagent chemotherapy versus 3 courses of high-dose cytarabine alone in postremission therapy for acute myeloid leukemia in adults: the JALSG AML201 Study

Shuichi Miyawaki,[1] Shigeki Ohtake,[2] Shin Fujisawa,[3] Hitoshi Kiyoi,[4] Katsuji Shinagawa,[5] Noriko Usui,[6] Toru Sakura,[1] Koichi Miyamura,[7] Chiaki Nakaseko,[8] Yasushi Miyazaki,[9] Atsushi Fujieda,[10] Tadashi Nagai,[11] Takahisa Yamane,[12] Masafumi Taniwaki,[13] Masatomo Takahashi,[14] Fumiharu Yagasaki,[15] Yukihiko Kimura,[16] Norio Asou,[17] Hisashi Sakamaki,[18] Hiroshi Handa,[19] Sumihisa Honda,[20] Kazunori Ohnishi,[21] Tomoki Naoe,[4] and Ryuzo Ohno[22]

[1]Leukemia Research Center, Saiseikai Maebashi Hospital, Maebashi, Japan; [2]Department of Clinical Laboratory Science, Kanazawa University Graduate School of Medical Science, Kanazawa, Japan; [3]Department of Hematology, Yokohama City University Medical Center, Yokohama, Japan; [4]Department of Hematology and Oncology, Nagoya University Graduate School of Medicine, Nagoya, Japan; [5]Hematology/Oncology Division, Okayama University Hospital, Okayama, Japan; [6]Division of Hematology and Oncology, Department of Internal Medicine, Jikei University School of Medicine, Tokyo, Japan; [7]Department of Internal Medicine, Japanese Red Cross Nagoya First Hospital, Nagoya, Japan; [8]Department of Hematology, Chiba University Hospital, Chiba, Japan; [9]Department of Hematology and Molecular Medicine Unit, Atomic Bomb Disease Institute, Nagasaki University Graduate School of Biomedical Sciences, Nagasaki, Japan; [10]Department of Hematology and Oncology, Mie University Graduate School of Medicine, Tsu, Japan; [11]Division of Hematology, Jichi Medical University, Shimotsuke, Japan; [12]Department of Hematology, Osaka City University, Osaka, Japan; [13]Department of Clinical Molecular Genetics and Laboratory Medicine, Kyoto Prefectural University of Medicine, Kyoto, Japan; [14]Division of Hematology and Oncology, Department of Internal Medicine, St Marianna University School of Medicine, Kawasaki, Japan; [15]Department of Hematology, Saitama Medical School, Hidaka, Japan; [16]Division of Hematology, First Department of Internal Medicine, Tokyo Medical University, Tokyo, Japan; [17]Department of Hematology, Kumamoto University School of Medicine, Kumamoto, Japan; [18]Department of Hematology, Tokyo Metropolitan Komagome Hospital, Tokyo, Japan; [19]Department of Medicine and Clinical Science, Gunma University Graduate School of Medicine, Maebashi, Japan; [20]Department of Public Health, Nagasaki University Graduate School of Biomedical Sciences, Nagasaki, Japan; [21]Oncology Center, Hamamatsu University School of Medicine, Hamamatsu, Japan; and [22]Aichi Cancer Center, Nagoya, Japan

We conducted a prospective randomized study to assess the optimal postremission therapy for adult acute myeloid leukemia in patients younger than 65 years in the first complete remission. A total of 781 patients in complete remission were randomly assigned to receive consolidation chemotherapy of either 3 courses of high-dose cytarabine (HiDAC, 2 g/m^2 twice daily for 5 days) alone or 4 courses of conventional standard-dose multiagent chemotherapy (CT) established in the previous JALSG AML97 study. Five-year disease-free survival was 43% for the HiDAC group and 39% for the multiagent CT group ($P = .724$), and 5-year overall survival was 58% and 56%, respectively ($P = .954$). Among the favorable cytogenetic risk group (n = 218), 5-year disease-free survival was 57% for HiDAC and 39% for multiagent CT ($P = .050$), and 5-year overall survival was 75% and 66%, respectively ($P = .174$). In the HiDAC group, the nadir of leukocyte counts was lower, and the duration of leukocyte less than 1.0×10^9/L longer, and the frequency of documented infections higher. The present study demonstrated that the multiagent CT regimen is as effective as our HiDAC regimen for consolidation. Our HiDAC regimen resulted in a beneficial effect on disease-free survival only in the favorable cytogenetic leukemia group. This trial was registered at www.umin.ac.jp/ctr/ as #C000000157. (*Blood*. 2011;117(8): 2366-2372)

Introduction

Approximately 70% to 80% of the newly diagnosed younger adult patients with acute myeloid leukemia (AML) achieve complete remission (CR) when treated with an anthracycline, usually daunorubicin (DNR) or idarubicin (IDR), and cytarabine (Ara-C); however, only approximately one-third of these patients remain free of disease for more than 5 years.[1-5] If CR patients are left untreated, almost all of them will relapse and die.[6] Therefore, postremission therapy is indispensable. Postremission therapy is divided into consolidation and maintenance therapy. In the previous studies of Japan Adult Leukemia Study Group (JALSG) for adult AML (AML87, 89, 92, and 95),[1-3,5] we administered 3 courses of consolidation therapy and 6 courses of intensified maintenance therapy. In the AML97 study,[7] we conducted a randomized study to compare the conventional 3-course consolidation and 6-course maintenance therapies with 4 courses of intensive consolidation therapy without maintenance and demonstrated no difference in overall survival (OS) and disease-free survival (DFS). Therefore, the 4 courses of conventional standard-dose multiagent chemotherapy (CT) became the standard regimen in Japan. On the other hand, multiple cycles of high-dose cytarabine (HiDAC) have been commonly used as consolidation therapy in the United States and other countries. However, our national medical insurance system did not allow us to use HiDAC until 2001, and thus we could not use HiDAC in the previous treatment regimens for leukemia. We therefore conducted this prospective, multicenter cooperative

Submitted July 6, 2010; accepted December 8, 2010. Prepublished online as *Blood* First Edition paper, December 29, 2010; DOI 10.1182/blood-2010-07-295279.

An Inside *Blood* analysis of this article appears at the front of this issue.

The publication costs of this article were defrayed in part by page charge payment. Therefore, and solely to indicate this fact, this article is hereby marked "advertisement" in accordance with 18 USC section 1734.

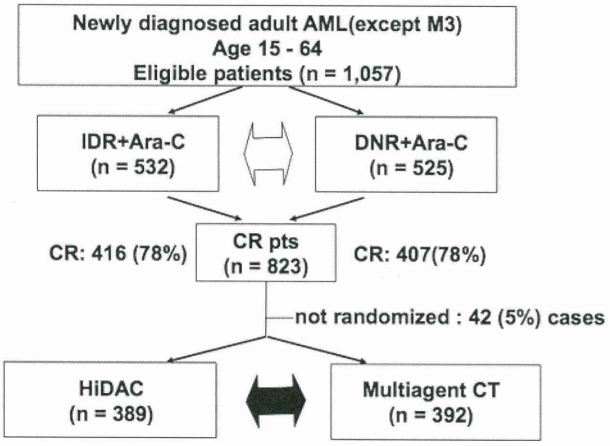

Figure 1. CONSORT diagram.

Table 1. Clinical characteristics of randomized patients

Characteristic	HiDAC (n = 389)	Multiagent CT (n = 392)	P
Age, y, median (range)	46 (15-64)	47 (15-64)	.697
WBC, $\times 10^9$/L, median (range)	15.6 (0.1-382)	14.9 (0.2-260)	.323
Karyotype, n			.210
Favorable	108	110	
Intermediate	242	256	
Adverse	27	14	
Unknown	12	12	
Induction, n			.914
IDR	196	196	
DNR	193	196	
Induction 1 cycle, %	81.0	81.4	.886

study to compare 4 courses of multiagent CT with 3 courses of HiDAC therapy after its approval in April 2001.

Methods

Patients

From December 2001 to December 2005, 1064 newly diagnosed adult patients 15 to 64 years of age with de novo AML were consecutively registered from 129 participating institutions. AML was first diagnosed by the French-American-British classification at each institution. Peripheral blood and bone marrow smears of registered patients were reevaluated by the central review committee. French-American-British M3 was not registered. Eligibility criteria included adequate function of liver (serum bilirubin < 2.0 mg/dL), kidney (serum creatinine < 2.0 mg/dL), heart and lung, and an Eastern Cooperative Oncology Group performance status between 0 and 3. Patients were not eligible if they had prediagnosed myelodysplastic syndrome or prior chemotherapy for other disorders. Cytogenetic abnormalities were grouped by standard criteria and classified according to the Medical Research Council classification.[8] The study was approved by institutional review boards at each participating institution. Written informed consent was obtained from all patients before registration in accordance with the Declaration of Helsinki.

Induction therapy consisted of Ara-C 100 mg/m^2 for 7 days and either IDR (12 mg/m^2 for 3 days) or DNR (50 mg/m^2 for 5 days). If patients did not achieve remission after the first course, the same therapy was administered once more. The outcome of induction therapy was reported to the JALSG Statistical Center before the consolidation therapy started. All CR patients were stratified according to induction regimen, number of courses of induction, age and karyotype, and randomized to receive either 4 courses of multiagent CT or 3 courses of HiDAC therapy. The first course of multiagent CT consisted of mitoxantrone (7 mg/m^2 by 30-minute infusion for 3 days) and Ara-C (200 mg/m^2 by 24-hour continuous infusion for 5 days). The second consisted of DNR (50 mg/m^2 by 30-minute infusion for 3 days) and Ara-C (200 mg/m^2 by 24-hour continuous infusion for 5 days). The third consisted of aclarubicin (20 mg/m^2 by 30-minute infusion for 5 days) and Ara-C (200 mg/m^2 by 24-hour continuous infusion for 5 days). The fourth consisted of Ara-C (200 mg/m^2 by 24-hour continuous infusion for 5 days), etoposide (100 mg/m^2 by 1-hour infusion for 5 days), vincristine (0.8 mg/m^2 by bolus injection on day 8), and vindesine (2 mg/m^2 by bolus injection on day 10). Each consolidation was started as soon as possible after neutrophils, white blood cells (WBCs), and platelets recovered to more than 1.5×10^9/L, 3.0×10^9/L, and 100.0×10^9/L, respectively. In the HiDAC group, 3 courses of Ara-C 2.0 g/m^2 by 3-hour infusion every 12 hours for 5 days were given. Each course was started 1 week after neutrophils, WBCs, and platelets recovered to the aforementioned counts.

Bone marrow examination was performed to confirm CR in both groups before each consolidation therapy and at the end of all consolidation therapy.

Best supportive care, including administration of antibiotics and platelet transfusions, was given if indicated. When patients had life-threatening documented infections during neutropenia, the use of granulocyte colony-stimulating factor was permitted.

After the completion of consolidation therapy, patients received no further chemotherapy. Allogeneic stem cell transplantation (allo-SCT) was offered during the first CR to patients of age 50 years or less with a histocompatible donor in the intermediate or adverse cytogenetic risk groups. Stem cell source was related donor or unrelated donor. Cord blood was not used. Conditioning before transplantation and prophylaxis for graft-versus-host disease were performed according to each institutional standard.

Responses were evaluated by the recommendations of the International Working Group.[9] CR was defined as the presence of all of the following: less than 5% of blasts in bone marrow, no leukemic blasts in peripheral blood, recovery of peripheral neutrophil counts more than 1.0×10^9/L and platelet counts more than 100.0×10^9/L, and no evidence of extramedullary leukemia. Relapse was defined as the presence of at least one of the

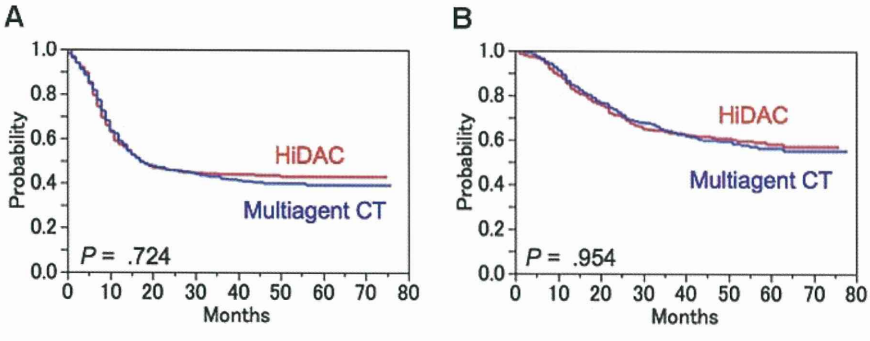

Figure 2. DFS and OS according to treatment arm. (A) DFS of CR patients. Predicted 5-year DFS was 43% for the HiDAC group (n = 389; red line) and 39% for the multiagent CT group (n = 392; blue line; $P = .724$). (B) OS of CR patients. Predicted 5-year OS was 58% for the HiDAC group (n = 389; red line) and 56% for the multiagent CT group (n = 392; blue line; $P = .954$).

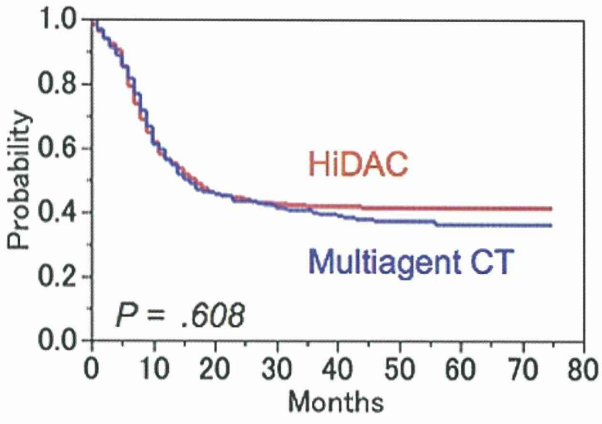

Figure 3. DFS according to treatment arm, after censoring the observation in transplanted patients. Predicted 5-year DFS was 41% for the HiDAC group (n = 389; red line) and 36% for the multiagent CT group (n = 392; blue line; $P = .608$).

following: reappearance of leukemic blasts in peripheral blood, recurrence of more than 5% blasts in bone marrow, and appearance of extramedullary leukemia.

Statistical analysis

This was a multi-institutional randomized phase 3 study with a 2 × 2 factorial design. The primary endpoint of the first randomization was CR rate, and a sample size of 420 patients per group was estimated to have a power of 90% at a 1% level of significance to demonstrate noninferiority (assuming 80% CR rate for both groups). For the second randomization (ie, this study), the primary endpoint was DFS, and the secondary end points were OS and adverse events of grade 3 or more by National Cancer Institute Common Toxicity Criteria. A sample size of 280 patients per group was estimated to have a power of 80% at a 5% level of significance to demonstrate 10% superiority in 5-year DFS for the HiDAC arm (40% vs 30%). OS was defined as the time interval from the date of diagnosis to the date of death. DFS for patients who had achieved CR was defined as the time interval from the date of CR to the date of the first event (either relapse or death). Patients who underwent allo-SCT were not censored. The Kaplan-Meier method was used to estimate probabilities of DFS and OS. For comparison of DFS and OS, the log-rank test was used for univariate analysis and the proportional hazard model of Cox for multivariate analysis. Cumulative incidence of relapse and treatment-related mortality were estimated according to the competing risk method and were evaluated with Gray test. The Wilcoxon rank-sum test was used for continuous data, such as age and WBC count, whereas the χ^2 test was used for ordinal data, such as risk group and frequency of allo-SCT. Statistical analyses were conducted using the JMP program (SAS Institute) and R software Version 2.9.1 (www.r-project.org).

Results

Response to induction therapy

Of 1064 patients registered, 1057 patients were evaluable. Seven patients (1 misdiagnosis, 1 infectious complication, 1 without therapy, and 4 withdrawal of consent) were excluded. Median age was 47 years (range, 15-64 years). Cytogenetic studies were performed in 99.2% of registered patients and the results were available in 97%. Of 1057 evaluable patients, 823 (78%) achieved CR (662 of them after the first induction course). CR rate in the IDR and DNR arms was similar (78.2% vs 77.5%). Percentage of patients who reached CR after the first induction course was also similar (64.1% vs 61.1%, $P = .321$). Day to achieve CR was longer in the IDR arm than the DNR arm (33.8 vs 32.4 days, $P = .038$). The detailed result of induction phase of this study is reported in a separate paper.[10]

Postremission randomization

Of 823 patients who achieved CR, 42 did not undergo the second randomization for a variety of reasons, which included residual toxicity from induction therapy (12), allo-SCT (8), death (1), refusal (1), and unknown (20). The remaining 781 patients were randomly assigned to receive either the HiDAC regimen (389) or the multiagent CT regimen (392; Figure 1). Clinical characteristics of 2 treatment groups were well balanced in age, initial WBC count, cytogenetic risk, induction arm, and induction cycle (Table 1).

DFS and OS

The median follow-up period of living patients was 48 months (range, 5-78 months). Five-year DFS was 43% for the HiDAC group and 39% for the multiagent CT group ($P = .724$; Figure 2A). Five-year OS was 58% for the HiDAC group and 56% for the multiagent CT group ($P = .954$; Figure 2B). After censoring the observation on the date of SCT in transplanted patients, 5-year DFS was 41% for the HiDAC group and 36% for the multiagent CT group ($P = .608$; Figure 3).

The cumulative incidences of relapse and treatment-related mortality during CR, respectively, were 49% and 8% for the HiDAC group and 56% and 5% for the multiagent CT group ($P = .294$, $P = .172$; Figure 4A). After censoring the observation in transplanted patients, those were 55% and 4% for the HiDAC group and 61% and 3% for the multiagent CT group ($P = .402$, $P = .409$), respectively (Figure 4B).

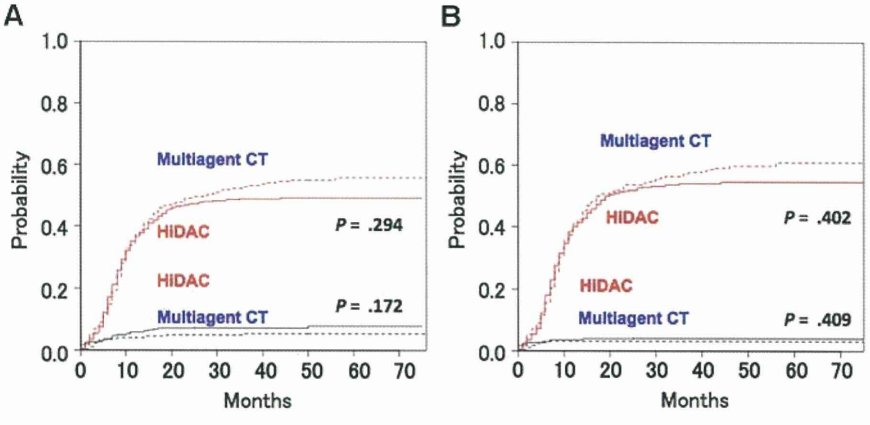

Figure 4. Cumulative incidence of relapse and treatment-related mortality in CR by treatment arm. (A) The incidences of relapse and mortality, respectively, were 49% and 8% for the HiDAC group (solid line) and 56% and 5% for the multiagent CT group (dotted line; $P = .324$, $P = .172$). (B) After censoring the observation in transplanted patients, the incidences of relapse and mortality, respectively, were 55% and 4% for the HiDAC group (solid line) and 61% and 3% for the multiagent CT group (dotted line; $P = .402$, $P = .409$).

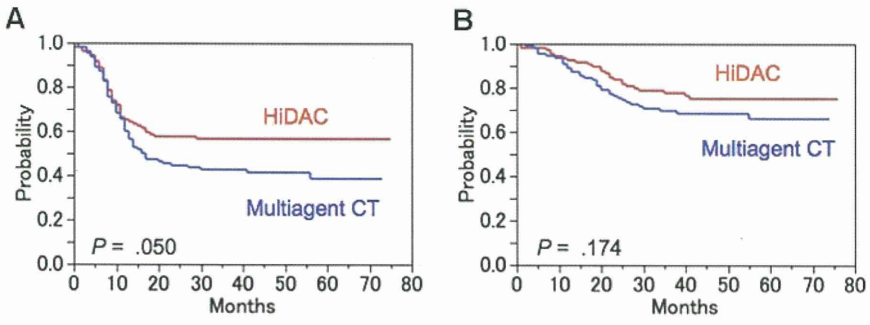

Figure 5. DFS and OS by treatment arm for the favorable cytogenetic risk group. (A) Predicted 5-year DFS was 57% for the HiDAC group (n = 108; red line) and 39% for the multiagent CT group (n = 110; blue line; $P = .050$). (B) Predicted 5-year OS was 75% for the HiDAC group (n = 108; red line) and 66% for the multiagent CT group (n = 110; blue line; $P = .174$).

In patients with the favorable cytogenetics, core-binding factor (CBF) leukemia with t(8;21) or inv(16), 5-year DFS was 57% in the HiDAC group and 39% in the multiagent CT group ($P = .050$; Figure 5A), and 5-year OS was 75% and 66%, respectively ($P = .174$; Figure 5B).

In patients with the intermediate cytogenetics, 5-year DFS was 38% in the HiDAC group and 39% in the multiagent CT group ($P = .403$; Figure 6A), and 5-year OS was 53% and 54%, respectively ($P = .482$; Figure 6B). In patients with the adverse cytogenetics, 5-year DFS was 33% in the HiDAC group and 14% in the multiagent CT group ($P = .364$; Figure 7A), and 5-year OS was 39% and 21%, respectively ($P = .379$; Figure 7B). Among younger patients ($\leq$ 50 years), 5-year DFS was 45% in the HiDAC group and 46% in the multiagent CT group ($P = .590$), and 5-year OS was 62% and 66%, respectively ($P = .228$). Among the older patients ($>$ 50 years), 5-year DFS was 40% in the HiDAC group and 28% in the multiagent CT group ($P = .230$), and 5-year OS was 51% and 40%, respectively ($P = .159$). In patients treated with the IDR regimen at induction, 5-year DFS was 42% in the HiDAC group and 41% in the multiagent CT group ($P = .641$), and 5-year OS was 58% and 57%, respectively ($P = .790$). In patients treated with the DNR regimen at induction, 5-year DFS was 44% in the HiDAC group and 37% in the multiagent CT group ($P = .339$), and 5-year OS was 58% and 56%, respectively ($P = .713$). There was no relationship between the duration of myelosuppression and DFS or OS.

Significant unfavorable prognostic features for DFS by the Cox proportional hazard model were WBC more than 20×10^9/L, the number of induction therapies, and age more than 50 years, and for OS, age more than 50 years, the number of induction therapies, WBC more than 20×10^9/L, and myeloperoxidase-positive blast less than 50%. Induction therapy, consolidation therapy, and cytogenetic risk group were not independent prognostic factors for DFS or OS by this multivariate analysis (Table 2).

Tolerance and toxicity of postremission therapy

All courses of consolidation were administered to 72.5% of patients in the HiDAC group and 70.2% in the multiagent CT group (Table 3). In the HiDAC group, 110 patients (28%) did not receive all 3 courses. The reasons included relapse (18), death in CR (10), allo-SCT (34), adverse events (27), patient's refusal (11), and unknown (10). In the multiagent CT group, 118 patients (30%) did not receive all 4 courses. The reasons included relapse (31), death in CR (8), allo-SCT (42), adverse events (13), patient's refusal (5), and unknown (19). The most common reason was allo-SCT in both groups. Of 125 patients received SCT in first CR, 49 (25 in HiDAC and 24 in multiagent CT) received SCT after completion of full courses of consolidation therapy. The second common reason was adverse events in the HiDAC group and relapse in the multiagent CT group. The patients older than 50 years could tolerate both regimens. Table 4 shows a comparison of both groups regarding the nadir of WBC count and the number of days of WBC less than 1.0×10^9/L. After each course of consolidation, the nadir of WBC count was significantly lower ($P < .0001$) and the day of WBC less than 1.0×10^9/L was significantly longer in the HiDAC group ($P < .001$). During each course of consolidation, the frequency and the number of days of granulocyte colony-stimulating factor administration were significantly higher in the HiDAC group. Table 5 shows toxic adverse events, excluding hematologic side effects. The frequency of documented infections was significantly higher in the HiDAC group ($P < .001$). The subset analysis showed the high incidence of documented infection in HiDAC regimen only in intermediate cytogenetic risk group ($P < .001$).

Discussion

To determine the best postremission therapy, there have been several prospective randomized studies comparing chemotherapy

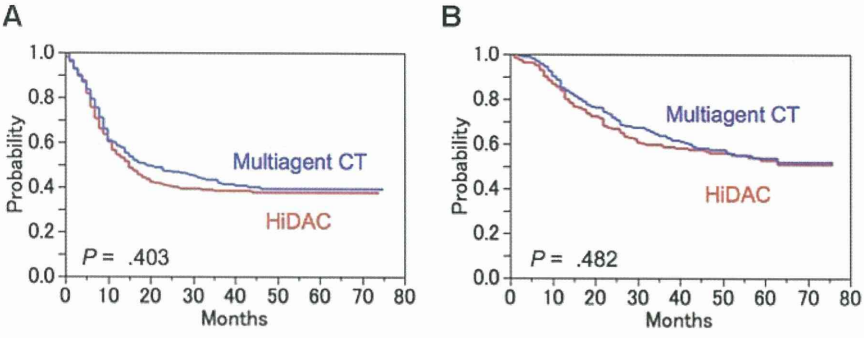

Figure 6. DFS and OS by treatment arm for the intermediate cytogenetic risk group. (A) Predicted 5-year DFS was 38% for the HiDAC group (n = 242; red line) and 39% for the multiagent CT group (n = 256; blue line; $P = .403$). (B) Predicted 5-year OS was 53% for the HiDAC group (n = 242; red line) and 54% for the multiagent CT group (n = 256; blue line; $P = .482$).

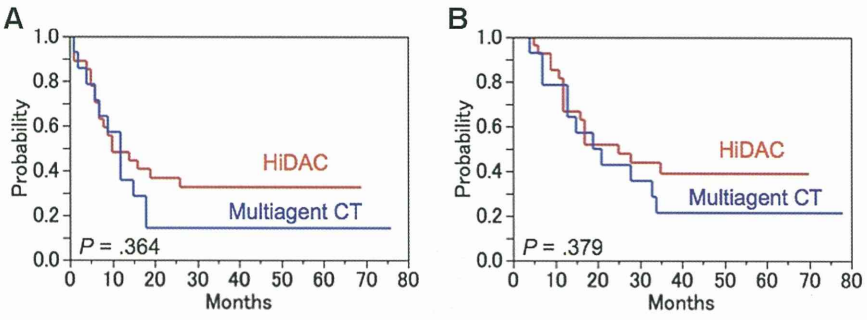

Figure 7. DFS and OS by treatment arm for the adverse cytogenetic risk group. (A) Predicted 5-year DFS was 33% for the HiDAC group (n = 27; red line) and 14% for the multiagent CT group (n = 14; blue line; $P = .364$). (B) Predicted 5-year OS was 39% for the HiDAC group (n = 27; red line) and 21% for the multiagent CT group (n = 14; blue line; $P = .379$).

with SCT. Although there is some limitation in SCT, such as patient age and availability of human leukocyte antigen–identical donors, most randomized studies demonstrate that SCT, the most intensive postremission modality, provides superior or at least noninferior prognosis in high- or intermediate-risk adult AML.[11-13]

As for postremission chemotherapy, HiDAC therapy is generally used in the United States and other countries after the landmark Cancer and Leukemia Group B-8525 (CALGB-8525) study.[14] In Japan, however, because HiDAC therapy was not approved by our national medical insurance system until 2001, combination chemotherapy using non–cross-resistant agents was commonly used in previous studies for adult AML. Therefore, in the current study, we compared conventional multiagent CT with HiDAC therapy.

Our study demonstrated that there is no difference in DFS and OS between the multiagent CT regimen and the HiDAC regimen. The HiDAC regimen, however, was accompanied with more frequent infectious events resulting from more severe and longer-lasting neutropenia. In the CALGB-8525 study,[14] patients randomized to 4 cycles of HiDAC regimen were administered 3 g/m^2 of Ara-C by 3-hour infusion, twice daily on days 1, 3, and 5, and our patients randomized to 3 cycles of HiDAC regimen were given 2 g/m^2 of Ara-C by 3-hour infusion, twice daily for 5 days. Although there were some differences in schedule and dose administered, the total dose of Ara-C was almost the same (72 g/m^2 vs 60 g/m^2). The Acute Leukemia French Association Group compared a timed-sequential consolidation consisting of etoposide, mitoxantrone, and Ara-C with a postremission chemotherapy, including 4 cycles of HiDAC (3 g/m^2), and reported that there were no statistically significant differences between the 2 groups in the rates of event-free survival and OS at 3 years.[15] The British Medical Research Council also compared a conventional Medical Research Council schedule (MACE/MidAC) with 2 courses of HiDAC regimens (3 g/m^2 or 1.5 g/m^2) and reported that there were no significant differences in DFS and OS at 5 years.[16]

On the contrary, the CALGB-8525 study[14] revealed that their HiDAC regimen was superior to the intermediate dose of Ara-C (400 mg/m^2 for 5 days) or to the conventional dose of Ara-C (100 mg/m^2 for 5 days) regimens in DFS and OS; this plausibly comes from the lower dose intensity of the intermediate- or standard-dose Ara-C regimens. Indeed, the CALGB-9222 study[17] showed no difference in DFS and OS between the HiDAC group and the intensified sequential multiagent chemotherapy group.

Cytogenetics is considered one of the most valuable prognostic determinants in adult AML.[8,18] In the present study, although in the intermediate-risk group, the DFS and OS of both consolidation groups were almost identical; in the favorable risk group, the outcome of the HiDAC group (n = 108) tended to be superior to that of the multiagent CT group (n = 110) in DFS (57% vs 39%; $P = .050$) and OS (75% vs 66%; $P = .174$) but not at statistically significant level; and in the adverse risk group, the similar but statistically nonsignificant trend in DFS (33% vs 14%) and OS (39% vs 21%) was noted. Bloomfield et al[19] reported that the HiDAC regimen is the most effective to CBF leukemia. In their study, patients with CBF leukemia (n = 18) had a 78% chance of remaining CR at 5 years when treated with the HiDAC regimen. However, our study showed that DFS of CBF leukemia (n = 108) treated with the HiDAC regimen was only 57% at 5 years.

There are 2 possible explanations of difference between our results and those reported by Bloomfield et al.[19] One is that their superior results may come from a small number of patients (n = 18). Indeed, the CALGB-9222 study,[17] including 28 patients with CBF leukemia, demonstrated that the 5-year DFS and OS of CBF leukemia treated with HiDAC was 60% and 70%, respectively. These data are similar to our results. The other is that CBF leukemia reveals different sensitivity to HiDAC therapy. Some patients with CBF abnormality have KIT mutations, which confer

Table 2. Factors to predict unfavorable prognostic features for DFS and OS by multivariate analysis

Survival type/variable	Category	Hazard ratio	*P*
DFS			
Initial WBC count	≥ 20 × 10^9/L	1.49	< .0001
No. of induction therapies	2 courses	1.50	.0006
Age, y	> 50	1.33	.0028
Consolidation therapy	Multiagent CT	1.04	.7128
OS			
Age, y	> 50	2.00	< .0001
No. of induction therapies	2 courses	1.58	.0033
Initial WBC count	≥ 20 × 10^9/L	1.41	.0070
MPO-positive blast	< 50 %	1.42	.0149
Consolidation therapy	Multiagent CT	0.96	.7768

MPO indicates myeloperoxidase.

Table 3. Tolerance of consolidation

	% receiving the full courses	
	HiDAC	Multiagent CT
All patients	72.5	70.2
Patients ≤ 50 y	71.9	69.0
Patients > 50 y	73.4	71.9
Reason for not receiving the full courses (no. of patients)		
Relapse	18	31
Death	10	8
SCT in first CR	31	42
Adverse event*	27	13
Patient refusal	11	5
Unknown	10	19

*$P < .05$.

Table 4. Intensity of consolidation

	HiDAC	Multiagent CT	*P*
After first consolidation			
Lowest WBC, $\times 10^9$/L	0.17	0.40	< .0001
Days WBC < 1.0 × 10^9/L	13 (0-40)	12 (0-36)	.0005
After second consolidation			
Lowest WBC, $\times 10^9$/L	0.10	0.40	< .0001
Days WBC < 1.0 × 10^9/L	14 (0-34)	13 (0-241)	.0007
After third consolidation			
Lowest WBC, $\times 10^9$/L	0.10	0.40	< .0001
Days WBC < 1.0 × 10^9/L	14 (0-38)	11.5 (0-28)	< .0001
After fourth consolidation			
Lowest WBC, $\times 10^9$/L		0.40	
Days WBC < 1.0 × 10^9/L		12 (0-34)	

Values are median (range).

higher relapse risk on CBF AML.[20,21] CALGB reported that 29.5% of patients with inv(16) and 22% of patients with t(8;21) had KIT mutations, and the cumulative incidence of relapse was higher for patients with mutated KIT than for those with wild-type KIT.[20] The difference of mutation rates of KIT might result in the difference in DFS. Unfortunately, in our present study, KIT mutations were not prospectively evaluated. However, a high mutation rate of KIT is reported among Asian patients with t(8;21) from Japan (37.8%)[22] and China (48.1%).[23] Consequently, JALSG is prospectively evaluating KIT mutation and its impact on the outcome in patients with CBF leukemia treated with repetitive HiDAC therapy. In the adverse cytogenetic risk group, the outcome of the HiDAC group also tends to be better than that of the multiagent CT group, but the difference is not statistically significant. The small number of this cohort may explain the statistical insignificance. Nevertheless, HiDAC therapy may be recommended to this group if patients have no human leukocyte antigen–matched donor.

Recently, IDR is frequently included into induction regimen for AML because of its better effectiveness compared with DNR.[24-26] A meta-analysis of randomized trials showed that the use of IDR instead of DNR results in a high CR rate.[27] However, a German group reported that the advantage of IDR in response rate may be lost during HiDAC consolidation therapy because of increased toxicity in the IDR group.[28] However, our current study demonstrated that, among the HiDAC group, there is no difference in DFS and OS between patients receiving IDR or DNR in induction phase. In our study, although one or 2 courses of the IDR regimen were given before the HiDAC consolidation, only 19% of patients required 2 courses to obtain CR. In contrast, the German group gave 2 courses of IDR induction regimen before the HiDAC consolidation. Thus, severe adverse events during HiDAC therapy probably depend on the total dose of prior IDR. Nevertheless, the HiDAC regimen could be given safely in our patients who had received IDR as induction therapy.

Table 5. Adverse events (CTC grades 3 and 4) during consolidation therapy

	HiDAC, %	Multiagent CT, %	*P*
Documented infection	20.9	14.5	< .001
Febrile neutropenia	66.5	66.4	.311
Bleeding	0.8	0.7	.601
Early death*	0.9	0.6	.389

*Death within 30 days after consolidation chemotherapy.

In conclusion, postremission consolidation regimen should be selected on the basis of prognostic factors, such as cytogenetics. Although several types of HiDAC regimen have been widely adopted as the optimal postremission therapy, the conventional multiagent CT may be recommendable for the intermediate or adverse cytogenetic risk groups. However, our HiDAC regimen should be recommended to the favorable cytogenetic risk group.

Acknowledgments

The authors thank the clinicians and the leaders of the 129 institutions who entered their patients into the JALSG AML201 study and provided the necessary data to make this study possible, as well as Miki Nishimura, who is recently deceased, for her major contributions to the design, conduct, and performance of this study.

This work was supported in part by grants from the Ministry of Health, Labor, and Welfare of Japan.

Authorship

Contribution: S.M. designed and performed research, interpreted data, and wrote the manuscript; S.O. designed and performed research, collected and analyzed data, and participated in writing the manuscript; S.F., H.K., K.S., N.U., T.S., K.M., C.N., Y.M., M. Taniwaki, T. Nagai, T.Y., A.F., M. Takahashi, F.Y., Y.K., N.A., H.S., H.H., S.H., K.O., and T. Naoe performed research; and R.O. interpreted data and participated in writing manuscript.

Conflict-of-interest disclosure: The authors declare no competing financial interests.

Correspondence: Shuichi Miyawaki, Division of Hematology, Tokyo Metropolitan Ohtsuka Hospital, 2-8-1 Minamiohtsuka, Toshima-ku, Tokyo, 170-8476, Japan; e-mail: miyawaki@mail.wind.ne.jp.

References

1. Ohno R, Kobayashi T, Tanimoto M, et al. Randomized study of individualized induction therapy with or without vincristine, and of maintenance-intensification therapy between 4 or 12 courses in adult acute myeloid leukemia: AML-87 Study of the Japan Adult Leukemia Study Group. *Cancer.* 1993;71(12):3888-3895.
2. Kobayashi T, Miyawaki S, Tanimoto M, et al. Randomized trials between behenoyl cytarabine and cytarabine in combination induction and consolidation therapy, and with or without ubenimex after maintenance/intensification therapy in adult acute myeloid leukemia. *J Clin Oncol.* 1996;14(1):204-213.
3. Miyawaki S, Tanimoto M, Kobayashi T, et al. No beneficial effect from addition of etoposide to daunorubicin, cytarabine, and 6-mercaptopurine in individualized induction therapy of adult acute myeloid leukemia: the JALSG-AML92 study. *Int J Hematol.* 1999;70(2):97-104.
4. Büchner T, Hiddemann W, Berdel WE, et al. 6-Thioguanine, cytarabine, and daunorubicin (TAD) and high-dose cytarabine and mitoxantrone (HAM) for induction, TAD for consolidation, and either prolonged maintenance by reduced monthly TAD or TAD-HAM-TAD and one course of intensive consolidation by sequential HAM in adult patients at all ages with de novo acute myeloid leukemia (AML): a randomized trial of the German AML Cooperative Group. *J Clin Oncol.* 2003;21(24):4496-4504.
5. Ohtake S, Miyawaki S, Kiyoi H, et al. Randomized trial of response-oriented individualized versus fixed-schedule induction chemotherapy with idarubicin and cytarabine in adult acute myeloid leukemia: the JALSG AML95 study. *Int J Hematol.* 2010;91(2):276-283.
6. Cassileth PA, Harrington DP, Hines JD, et al. Maintenance chemotherapy prolongs remission duration in adult acute nonlymphocytic leukemia. *J Clin Oncol.* 1988;6(4):583-587.
7. Miyawaki S, Sakamaki H, Ohtake S, et al. A randomized, postremission comparison of four courses of standard-dose consolidation therapy without maintenance therapy versus three courses of standard-dose consolidation with maintenance therapy in adults with acute myeloid leukemia. *Cancer.* 2005;104(12):2726-2734.

8. Grimwade D, Walker H, Oliver F, et al. The importance of diagnostic cytogenetics on outcome in AML: analysis of 1612 patients entered into the MRC AML 10 trial. *Blood.* 1998;92(7):2322-2333.
9. Cheson BD, Bennett JM, Kopecky KJ, et al. Revised recommendations of the International Working Group for Diagnosis, Standardization of Response Criteria, Treatment Outcomes, and Reporting Standards for Therapeutic Trials in Acute Myeloid Leukemia. *J Clin Oncol.* 2003; 21(24):4642-4649.
10. Ohtake S, Miyawaki S, Fujita H, et al. Randomized study of induction therapy comparing standard-dose idarubicin with high-dose daunorubicin in adult patients with previously untreated acute myeloid leukemia: JALSG AML201 Study. *Blood.* 2011;117(8):2357-2364.
11. Zittoun RA, Mandelli F, Willemze R, et al. Autologous or allogeneic bone marrow transplantation compared with intensive chemotherapy in acute myeloid leukemia. *N Engl J Med.* 1995;332(4): 217-223.
12. Burnett AK, Wheatley K, Goldstone AH et al. The value of allogeneic bone marrow transplant in patients with acute myeloid leukaemia at differing risk of relapse: results of the UK MRC AML 10 trial. *Br J Haematol.* 2002;118(2):385-400.
13. Sakamaki H, Miyawaki S, Ohtake S, et al. Allogeneic stem cell transplantation versus chemotherapy as post-remission therapy for intermediate or poor risk adult acute myeloid leukemia: results of the JALSG AML97 study. *Int J Hematol.* 2010;91(2):284-292.
14. Mayer RJ, Davis RB, Schiffer CA, et al. Intensive postremission chemotherapy in adults with acute myeloid leukemia. *N Engl J Med.* 1994;331(14): 896-903.
15. Thomas X, Raffoux E, Botton S et al. Effect of priming with granulocyte-macrophage colony-stimulating factor in younger adults with newly diagnosed acute myeloid leukemia: a trial by the Acute Leukemia French Association (ALFA) Group. *Leukemia.* 2007;21(3):453-461.
16. Burnett AK, Hills RK, Milligan D, et al. Attempts to optimise induction and consolidation chemotherapy in patients with acute myeloid leukaemia: results of the MRC AML15 trial [abstract]. *Blood.* 2009;114(22):200. Abstract 484
17. Moore JO, George SL, Dodge RK, et al. Sequential multiagent chemotherapy is not superior to high-dose cytarabine alone as postremission intensification therapy for acute myeloid leukemia in adults under 60 years of age: Cancer and Leukemia group B study 9222. *Blood.* 2005;105(9): 3420-3427.
18. Slovak ML, Kopecky KJ, Cassileth PA et al. Karyotypic analysis predicts outcome of preremission and postremission therapy in adult acute myeloid leukemia: a Southwest Oncology Group/Eastern Cooperative Oncology Group study. *Blood.* 2000;96(13):4075-4083.
19. Bloomfield CD, Lawrence D, Byrd JC, et al. Frequency of prolonged remission duration after high-dose cytarabine intensification in acute myeloid leukemia varies by cytogenetic subtype. *Cancer Res.* 1998;58(18):4173-4179.
20. Paschka P, Marcucci G, Ruppert AS, et al. Adverse prognostic significance of KIT mutations in adult acute myeloid leukemia with inv(16) and t(8;21): a Cancer and Leukemia Group B Study. *J Clin Oncol.* 2006;24(24):3904-3911.
21. Cairoli R, Beghini A, Grillo G, et al. Prognostic impact of c-KIT mutations in core binding factor leukemias: an Italian retrospective study. *Blood.* 2006;107(9):3463-3468.
22. Nanri T, Matsuno N, Kawakita T, et al. Mutations in the receptor tyrosine kinase pathway are associated with clinical outcome in patients with acute myeloblastic leukemia harboring t(8;21)(q22; q22). *Leukemia.* 2005;19(8):1361-1366.
23. Wang YY, Zhou GB, Yin T, et al. AML1-ETO and C-KIT mutation/overexpression in t(8;21) leukemia: implication in stepwise leukemogenesis and response to Gleevec. *Proc Natl Acad Sci U S A.* 2005;102(4):1104-1109.
24. Berman E, Heller G, Santorsa J, et al. Results of a randomized trial comparing idarubicin and cytosine arabinoside with daunorubicin and cytosine arabinoside in adult patients with newly diagnosed acute myelogenous leukemia. *Blood.* 1991;77(8):1666-1674.
25. Wiernik PH, Banks PL, Case DC Jr, et al. Cytarabine plus idarubicin or daunorubicin as induction and consolidation therapy for previously untreated adult patients with acute myeloid leukemia. *Blood.* 1992;79(2):313-319.
26. Vogler WR, Velez-Garcia E, Weiner RS, et al. A phase III trial comparing idarubicin and daunorubicin in combination with cytarabine in acute myelogenous leukemia: a Southeastern Cancer Study Group Study. *J Clin Oncol.* 1992;10(7): 1103-1111.
27. AML Collaborative Group. A systematic collaborative overview of randomized trials comparing idarubicin with daunorubicin (or other anthracyclines) as induction therapy for acute myeloid leukaemia. *Br J Haematol.* 1998;103(1):100-109.
28. Seipelt G, Hofmann WK, Martin H, et al. Comparison of toxicity and outcome in patients with acute myeloid leukemia treated with high-dose cytosine arabinoside consolidation after induction with a regimen containing idarubicin or daunorubicin. *Ann Hematol.* 1998;76(3):145-151.

Open

Leukemia (2011) 25, 575–587

www.nature.com/leu

ORIGINAL ARTICLE

LBH589, a deacetylase inhibitor, induces apoptosis in adult T-cell leukemia/lymphoma cells via activation of a novel RAIDD-caspase-2 pathway

H Hasegawa[1], Y Yamada[1], K Tsukasaki[2], N Mori[3], K Tsuruda[1], D Sasaki[1], T Usui[1], A Osaka[1], S Atogami[1], C Ishikawa[3,4], Y Machijima[3], S Sawada[3], T Hayashi[5], Y Miyazaki[2] and S Kamihira[1]

[1]*Department of Laboratory Medicine, Nagasaki University Graduate School of Biomedical Sciences, Nagasaki, Japan;* [2]*Department of Hematology, Atomic Disease Institute, Nagasaki University Graduate School of Biomedical Sciences, Nagasaki, Japan;* [3]*Division of Molecular Virology and Oncology, Graduate School of Medicine, University of the Ryukyus, Nishihara, Okinawa, Japan;* [4]*Transdisciplinary Research Organization Subtropics Island Studies, University of the Ryukyus, Nishihara, Okinawa, Japan and* [5]*Department of Pathology, Nagasaki University Hospital, Nagasaki, Japan*

Adult T-cell leukemia/lymphoma (ATLL), an aggressive neoplasm etiologically associated with human T-lymphotropic virus type-1 (HTLV-1), is resistant to treatment. In this study, we examined the effects of a new inhibitor of deacetylase enzymes, LBH589, on ATLL cells. LBH589 effectively induced apoptosis in ATLL-related cell lines and primary ATLL cells and reduced the size of tumors inoculated in SCID mice. Analyses, including with a DNA microarray, revealed that neither death receptors nor p53 pathways contributed to the apoptosis. Instead, LBH589 activated an intrinsic pathway through the activation of caspase-2. Furthermore, small interfering RNA experiments targeting caspase-2, caspase-9, RAIDD, p53-induced protein with a death domain (PIDD) and RIPK1 (RIP) indicated that activation of RAIDD is crucial and an event initiating this pathway. In addition, LBH589 caused a marked decrease in levels of factors involved in ATLL cell proliferation and invasion such as CCR4, IL-2R and HTLV-1 HBZ-SI, a spliced form of the HTLV-1 basic zipper factor HBZ. In conclusion, we showed that LBH589 is a strong inducer of apoptosis in ATLL cells and uncovered a novel apoptotic pathway initiated by activation of RAIDD.
Leukemia (2011) **25,** 575–587; doi:10.1038/leu.2010.315;
published online 18 January 2011
Keywords: LBH589; apoptosis; adult T-cell leukemia; caspase-2; RAIDD

Introduction

There is evidence that gene expression governed by epigenetic changes is crucial to the pathogenesis of cancer.[1] Histone deacetylases are enzymes involved in the remodeling of chromatin, and have a key role in the epigenetic regulation of gene expression. In addition, the activity of non-histone proteins can be regulated through histone deacetylase-mediated hypoacetylation.[2] Deacetylase inhibitors (DACi) induce the hyperacetylation of non-histone proteins, as well as nucleosomal histones resulting in the expression of repressed genes involved in growth arrest, terminal differentiation and/or apoptosis among cancer cells.[3,4] Several classes of DACi have been found to have potent anticancer effects in preclinical studies.[2] Despite a consensus on the importance of apoptosis to the effect of these drugs, different apoptotic mechanisms have been reported.[2] For instance, even the contribution of caspases to DACi-induced apoptosis is quite controversial.[5–8]

Correspondence: Dr Y Yamada, Department of Laboratory Medicine, Nagasaki University Graduate School of Biomedical Sciences, 1-7-1 Sakamoto, Nagasaki City 852-8501, Japan.
E-mail: y-yamada@nagasaki-u.ac.jp
Received 1 April 2010; revised 24 November 2010; accepted 10 December 2010; published online 18 January 2011

There are two general apoptotic pathways, the receptor (extrinsic) pathway and the mitochondrial (intrinsic) pathway.[9] The extrinsic pathway requires activation of caspase-8, which results in activation of the zymogens of executioner caspases such as caspase-3, eventually leading to cleavage of poly ADP-ribose polymerase (PARP). Proteolytic caspase-8 can further activate BH3-interacting domain death agonist (BID), and cleaved BID moves to the mitochondria where it triggers the release of cytochrome-*c*. In the intrinsic pathway, death signals lead to changes in the mitochondrial outer membrane's permeability, subsequently releasing cytochrome-*c*, which forms an apoptosome with caspase-9, eventually activating executioner caspases.[10]

LAQ824 and the more potent and newly developed DACi analog LBH589 are now under clinical investigation as a therapeutic agent for several kinds of cancer.[2,4] One unique feature of these drugs is their role in the regulation of heat shock protein 90kDa-α (HSP90) and degradation of HSP90 client proteins such as bcr–abl in chronic myelogenous leukemia and fms-related tyrosine kinase 3 in acute myeloid leukemia.[11–15]

Adult T-cell leukemia/lymphoma (ATLL) is a neoplasm of mature T-lymphocyte origin etiologically associated with human T-lymphotropic virus type-1 (HTLV-1) and is known to be resistant to standard anticancer therapies.[16] Previous findings suggest that the viral protein HTLV-1 Tax interferes with most DNA repair mechanisms, preventing cell cycle arrest and apoptosis, and contributing to the early stages of ATLL.[17,18] In addition, the novel viral protein HTLV-1 basic zipper factor (HBZ) and its spliced form (HBZ SP1RNA or HBZ-SI), which are encoded by the minus-strand RNA of the HTLV-1 genome, have been identified recently.[19–23] These proteins are thought to be functional and expected to be closely involved in the late stages of ATLL.[24] ATLL is generally classified into four clinical subtypes: acute, chronic, smoldering and lymphoma. Although several approaches have been reported, combination chemotherapy is still the treatment of choice for newly diagnosed acute and lymphoma-type ATLL. Patients with aggressive ATLL have a median survival period of 13 months, indicating limitations in the treatment of ATLL.[25,26] In this study, we examined the effects of LBH589 on ATLL cells *in vitro* and *in vivo*, and investigated the pathways or factors contributing to the LBH589-induced ATLL cell death.

Materials and methods

Cell preparation

The ATLL-derived cell lines ST1, KOB, LM-Y1, LM-Y2, KK1 and SO4 were established in our laboratory from ATLL patients[27,28] and maintained in RPMI 1640 medium supplemented with

10% fetal bovine serum and 0.5 U/ml of interleukin-2 (kindly provided by Takeda Pharmaceutical Company, Ltd., Osaka, Japan). The HTLV-1-infected T-cell lines MT2 and HuT102,[29,30] human T-cell leukemia cell line Jurkat and erythromyeloblastoid cell line K562 were maintained in RPMI 1640 medium supplemented with 10% fetal bovine serum. The ST1, KOB, LM-Y1, MT2 and HuT102 cells have the wild-type p53.[31] Primary leukemia cells from eight patients with acute-type ATLL were also analyzed. The diagnosis of ATLL and preparation of peripheral blood mononuclear cells from patients with ATLL and normal healthy donors were described previously.[28] Each patient's sample contained more than 80% leukemia cells at the time of analysis. After approval by the Ethics Committee at Nagasaki University Hospital, all materials from patients were obtained with informed consent.

Chemicals and cell proliferation assay

Chemicals used in this study were LBH589 (kindly provided by Novartis Pharma AG., Basel, Switzerland), SAHA (Cayman Chemical, Ann Arbor, MI, USA), MG132 (Biomol Research Laboratories, Plymouth Meeting, PA, USA), LY294002 (Biomol), soluble tumor necrosis factor related apoptosis-inducing ligand (TRAIL) (Biomol), staurosporine (Merck, Darmstadt, Germany), the pan-caspase inhibitor z-VAD-fmk, the caspase-2 inhibitor Z-VDVAD-fmk and the caspase-9 inhibitor Z-LEHD (MBL, Nagoya, Japan). The cell proliferation assay (3-(4,5-dimethylthiazol-2-yl)-5-(3-carboxymethoxyphenyl)-2-(4-sulfophenyl)-2H-tetrazolium, inner salt assay) was performed with a Cell Titer 96 AQueos Cell Proliferation Assay kit (Promega, Madison, WI, USA) according to the manufacturer's directions.

In vivo *experiments using SCID mice*

Five-week-old female C.B-17/Icr-SCID mice obtained from Ryukyu Biotec (Urasoe, Japan) were maintained in containment level 2 cabinets and provided with autoclaved food and water *ad libitum*. The mice were engrafted with 10^7 HuT102 cells by subcutaneous injection in the post-auricular region and randomly placed into two cohorts of five animals each that received vehicle or LBH589. Treatment was initiated on the day after cell injection. LBH589 was dissolved in distilled water at a concentration of 2 mg/ml, and 28 mg/kg body weight of LBH589 was administered by oral gavage three times a week. Control mice received the same volume of the vehicle only. Body weight and tumor numbers and size were monitored once a week. All mice were sacrificed on day 28, then the tumors were dissected out, and their weight was measured. After tumors were fixed for paraffin embedding and tissue sectioning, DNA fragmentation was evaluated by fluorescent TUNEL (TAKARA BIO INC., Shiga, Japan) as recommended by the manufacturer. All these experiments were performed according to the Guidelines for Animal Experimentation of the University of the Ryukyus and were approved by the Animal Care and Use Committee of the same university.

Flow cytometric analysis

To evaluate apoptotic changes and the permeability of the mitochondrial outer membrane, we used an Annexin-V and PI Kit (Bender Medsystems, Vienna, Austria) and a Mitochondrial Membrane Potential Assay Kit (5, 5′, 6, 6′-tetrachloro-1, 1′, 3, 3′-tetraethylbenzimidazol-carbocyanine iodide detection) (Cayman Chemical), respectively. Activities of caspase-8 and 9 were determined by fluorometric assay (MBL) according to the manufacturer's instructions. The cell-surface expression of death receptors (DRs), CCR4 and IL-2R was examined by flow cytometric analysis using anti-tumor necrosis factor-R1 (MBL), anti-CD95 (BD Biosciences, San Diego, CA, USA), anti-DR5 (Alexis Biochemicals, San Diego, CA, USA), anti-CCR4 (BD) and anti-CD25 (BD) monoclonal antibodies. Mouse IgG1 (DAKO, Kyoto, Japan) was used as a negative control. All experiments were performed using a FACSCalibur flowcytometer and Cellquest software (BD).

Preparation of whole-cell lysate, nuclear, mitochondrial and cytosolic fractions

Cells were harvested after treatment and whole-cell lysate was prepared as described previously.[32] Nuclear extracts from cells were prepared for NF-κB transcription assays using a nuclear/cytosol fractionation kit (BioVision, San Diego, CA, USA), according to the instructions. Similarly, cytosolic fractions were prepared for western blotting by using a mitochondria/cytosol fractionation kit (BioVision).

Western blotting, immunoprecipitation and antibodies

Western blotting was performed as described previously.[31] The analysis was performed using antibodies to p53 (DO-1), MDM2 (Ab-1), FADD, PUMA and NOXA (Merck), phospho-AKT, AKT, caspase-8, 9 and 3, cleaved caspase-9, cleaved PARP, BID, BAX, Bcl-xL, cytochrome-c, p21 and acetylated-Lysin (Cell Signaling Technology, Beverly, MA, USA), p53-induced protein with a death domain (PIDD) (LifeSpan Biosciences, Seattle, WA, USA), caspase-2 (11B4) and c-FLIP (Dave-2) (Alexis), RAIDD and TRADD (MBL), survivin (R&D systems Inc., Minneapolis, MN, USA), acetylated-histone-H3 and -H4, and Bcl-2 (Upstate Biotechnology, Waltham, MA, USA), RIP and XIAP (BD), HBZ (kindly provided by Dr JM Mesnard) and HBZ-SI,[22] Tax,[31] acetylated-tubulin, α-tubulin and β-actin (Sigma Chemicals, St Louis, MO, USA). In the immunoprecipitation assay, protein A-Sepharose beads (Sigma), HSP90 antibody (StressGen Biotechnologies Corporation, Victoria, BC, Canada) and RAIDD antibody (LifeSpan Biosciences) were used.

Immunohistochemistry

After tumors were fixed for paraffin embedding and tissue sectioning, immunohistochemical staining for acetylated-histone-H3 and -H4 was performed. The deparaffinized slides were pretreated with DAKO Target Retrival Solution (pH 9) (DAKO), and heated in a water bath at 95 °C for 40 min. For all stains, the endogenous peroxidase was quenched by 3% H_2O_2 for 15 min. Sections were then placed in 0.5% nonfat dry milk for 30 min at room temperature. The primary antibodies used were anti-acetylated-histone-H3 and -H4 (Cell Signaling). They were allowed to react for 1 h at room temperature, and then the DAKO EnVision + Dual Link System-HRP (DAKO) was applied using diaminobenzidine as the chromogen, following the manufacturer's directions.

Proteasome activity assay

The proteolytic activity of the 20S proteasome was evaluated with the Biomol AK-740 QuantiZyme Assay System (Biomol) following the manufacturers' instructions, which detects the release of the free 7-amino-4-methylcoumarin fluorophore, upon cleavage of the fluorogenic peptide Suc-LLVYAMC.

DNA microarray analysis

Total RNA from cells was extracted using ISOGEN (Nippon Gene, Toyama, Japan) and purified with a Message Clean kit

(GenHunter Corp., Brookline, MA, USA). The RNA's integrity was assessed using an Agilent 2100 Bioanalyzer (Agilent, Palo Alto, CA, USA). Double-stranded cDNA and biotinylated cRNA were synthesized using a T7-poly-T primer and the BioArray RNA labeling kit (Enzo, Farmingdale, NY, USA), respectively. The labeled RNA was then fragmented and hybridized to HU-133A oligonucleotide arrays (Affymetrix, Santa Clara, CA, USA). The arrays were scanned using the Gene Array Scanner and analyzed using the DNA-Chip Analyzer.

Real-time quantitative RT-PCR

After total RNA was prepared as described above, Real-time RT-PCR for HBZ, HBZ-SI and Tax were performed using a LightCycler Technology System (Roche Diagnostics, Basel, Switzerland) as described previously.[22,28,33] Similarly, PCRs for caspase-2, caspase-9, RAIDD, PIDD and PBGD were performed on a Roche LC480 (Roche) with LightCycler 480 Probes Master mix (Roche) according to the directions. We designed specific sets of primers and/or purchased probes as summarized in Supplementary Table 1.

NF-κB transcription factor assay

Nuclear extracts from cells were prepared as described above. Activities of NF-κB p50 and p65 were investigated using an NF-κB transcription factor assay kit (Chemicon, Temecula, CA, USA) as recommended by the manufacturer.

Transfection, luciferase assay and small interfering RNA experiments

Transfection was performed with a Cell line Nucleofector kit V and the Nucleofector system (Lonza, Cologne, Germany). The transfection programs for ST1 (O-17) and HuT102 (O-16) were determined so that the viability of cells and the transfection efficiency would be compatible (data not shown). Luciferase assays using reporter plasmid pG13-Luc were described previously.[31] The plasmid Myr-AKT (pcDNA3 myr-HA-Akt1) was obtained from Addgene Inc. (Cambridge, MA, USA).[34] Empty pcDNA3 or Myr-AKT vectors were used for the AKT-transfection experiment. Cells (5×10^6) were resuspended in 100 μl of Cell line Nucleofector solution V and mixed with 2 μg of plasmid DNA. Twenty-four hours after transfection, the cells were cultured with or without LBH589 and processed for flow cytometric analysis or western blotting. We prepared three different small interfering RNA (siRNA) against each target. Caspase-2: Silencer Select Validated siRNA s2412 (#1), s2410 (#2) and s2411 (#3), caspase-9: Silencer Select siRNA s2430 (#1), s2428 (#2) and s2429 (#3), RAIDD: Silencer Select siRNA s16656 (#1), s16654 (#2) and s16655 (#3), PIDD: Silencer Select siRNA s30843 (#1), s30844 (#2) and s226845 (#3), RIP: Silencer Select Validated siRNA s16651 (#1), s11652 (#2) and s16653 (#3), and control siRNA (Silencer negative control #1) (Applied Biosystems, Foster City, CA, USA). After evaluating the effect of each siRNA by monitoring the target's mRNA and protein (Supplementary Figure 2), we eventually selected a set of #1 siRNA against each target. Cells were used 24 h after transfection and each siRNA experiment was performed in triplicate.

Results

LBH589 causes acetylation of histones and non-histone proteins in ATLL cells

Hydroxamate-based DACi including LBH589 induce hyperacetylation of histones H3/H4 and α-tubulin.[2,4] Recent reports also indicated that LAQ824 and LBH589 can cause acetylation of HSP90 and the disruption of its chaperone function, resulting in repression of HSP90 client proteins including AKT.[12,35] We first confirmed that LBH589 was very effective in increasing the acetylation of histones H3/H4 and α-tubulin in ATLL-related cell lines (Figure 1a). As expected, LBH589 also caused acetylation of HSP90 in ST1, KOB and KK1 cells and significantly reduced the expression of phospho-AKT (Figures 1b and c).

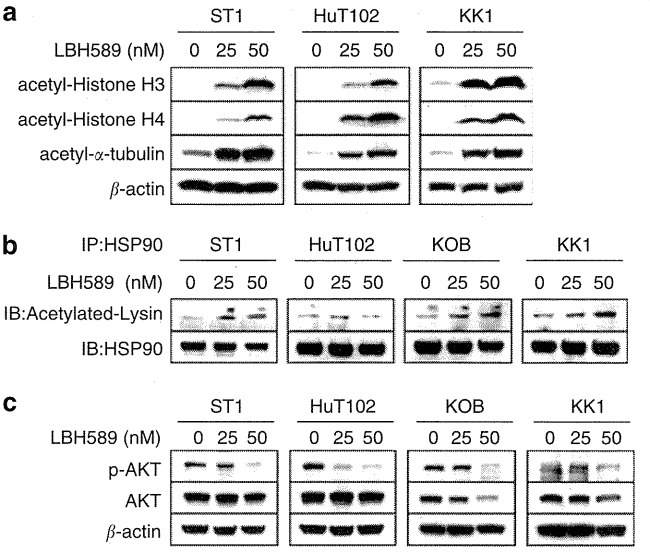

Figure 1 LBH589 causes acetylation of histones and non-histone proteins in adult T-cell leukemia/lymphoma (ATLL) cells. Cells were treated with either vehicle or the indicated concentrations of LBH589 for 24 h. Whole-cell lysate was prepared, and (**a** and **c**) western blotting was performed. (**b**) For each sample, 100 μg of cell lysate was used for immunoprecipitation with a monoclonal antibody to heat shock protein 90kDa α (HSP-90), and western blotting was performed.

LBH589 induces apoptosis in ATLL cells

Next, we examined the effect of LBH589 on the growth of 8 ATLL-related cell lines, Jurkat cells and K562 cells. LBH589 caused ~60% inhibition of cell growth at a concentration of 25 nM in the ATLL-related cell lines and Jurkat cells, and about 30% inhibition in the K562 cells (Figure 2a). ST1, HuT102 and MT2 cells were especially sensitive with more than 60% of their growth inhibited at 12 nM. To determine the details of LBH589-mediated cell death, we performed Annexin-V/PI staining. After 48-h treatment with 25 nM of LBH589, Annexin-V-positive cells in the ST1 and HuT102 cell lines increased from 8 and 4% to 71 and 92%, respectively (Figure 2b). Likewise, more than 30% of cells were positive for Annexin-V after 24-h treatment with 25 nM of LBH589 in the other cell lines except K562, in which the proportion was 9.5% (Figure 2c). These results indicate that ATLL-related cell lines are highly sensitive to LBH589-induced apoptosis. Similar to the results for the cell lines, LBH589 significantly inhibited cell proliferation in all primary ATLL cell samples examined. In contrast, normal peripheral blood mononuclear cells were less harmed than ATLL cells (Figure 2d). Annexin-V/PI staining confirmed that LBH589 induces apoptotic cell death in primary ATLL cell samples (Figure 2e).

Treatment of subcutaneous tumors with LBH589

We examined whether LBH589 is also effective against ATLL cells in the *in vivo* setting, by using SCID mice transplanted with HuT102 cells. Ten mice were inoculated, five of which were

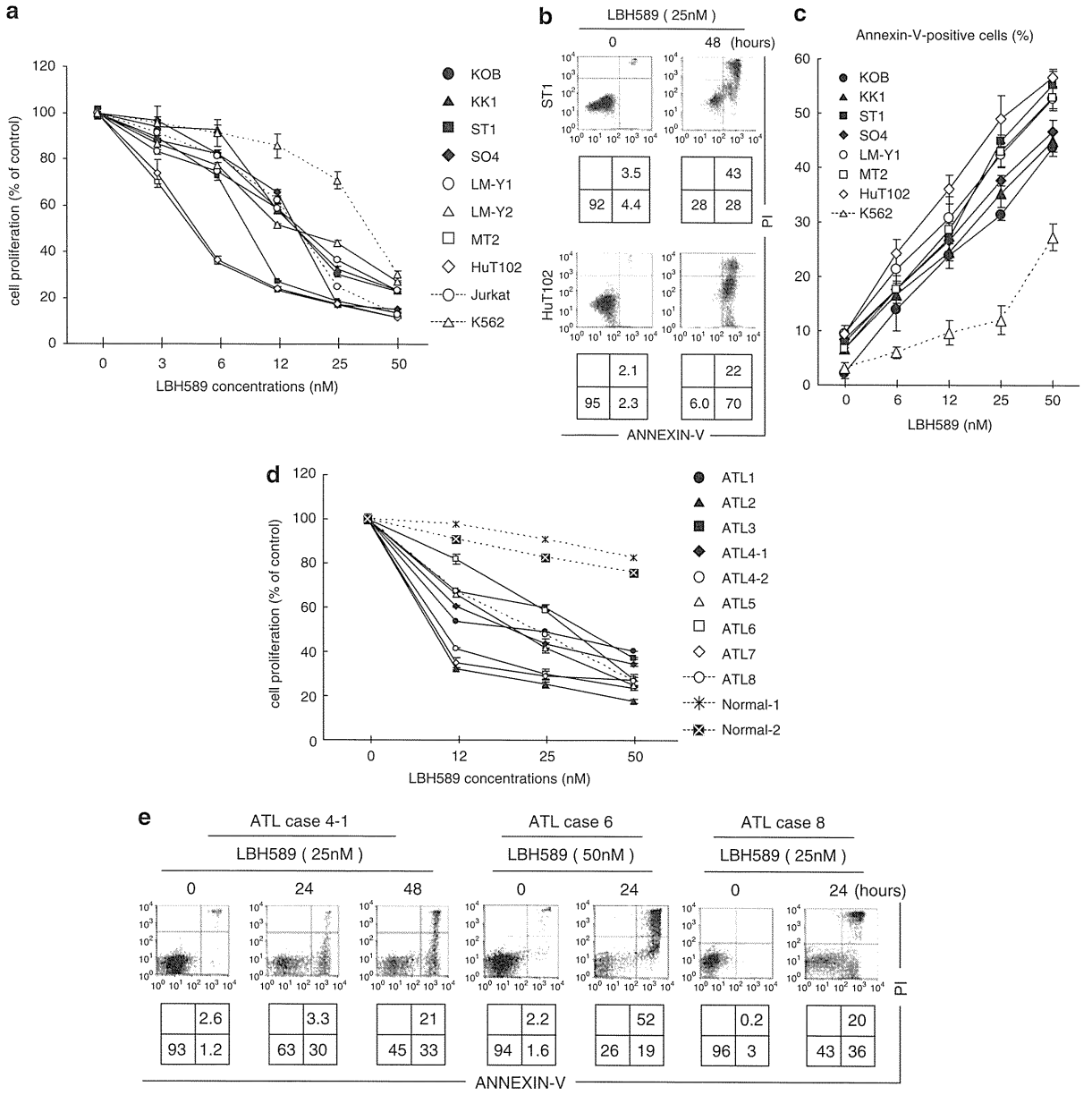

Figure 2 LBH589 induces apoptosis in adult T-cell leukemia/lymphoma (ATLL)-related cell lines and primary ATLL cells. (**a** and **d**) Cell lines ($3–5 \times 10^5$/ml), primary ATLL cells or normal peripheral blood mononuclear cell (PBMCs) ($7–10 \times 10^5$/ml) were treated with either vehicle or the indicated concentrations of LBH589 for 48 h and cell proliferation (% against cells cultured without LBH589) was evaluated by MTS (3-(4, 5-dimethylthiazol-2-yl)-5-(3-carboxymethoxyphenyl)-2-(4-sulfophenyl)-2H-tetrazolium, inner salt) assay. (**b**, **c** and **e**) After cells were treated with the indicated concentrations and time course, Annexin-V/PI staining was performed. (**b** and **e**) Percentages of intact cells (Annexin-V^- PI^-), early apoptotic cells (Annexin-V^+ PI^-) and late apoptotic or necrotic cells (Annexin-V^+ PI^+) are indicated in the lower panels. (**c**) Percentages of Annexin-V-positive cells were evaluated. (**a**, **c** and **d**) Experiments were performed in triplicate and results were expressed as the mean ± s.d. In ATLL case 4, samples from peripheral blood mononuclear cells (4–1) and pleural effusion (4–2) were investigated.

treated with LBH589 and five of which were left untreated. LBH589 reduced the volume of tumors more than 70% (Figure 3a). The mean tumor weight of LBH589-treated mice was significantly lower than that of control mice (Figure 3b). Immunohistochemical staining confirmed that LBH589 was very effective in increasing the acetylation of histones H3/H4 in tumors of treated mice (Figure 3c). We further confirmed by a TUNEL assay that LBH589 caused evident apoptosis in transplanted tumors (Figure 3d).

Analysis of the extrinsic pathway in LBH589-induced apoptosis

DACi are reported to activate the extrinsic pathway, in many cases, in cooperation with (DRs).[2] Among typical DRs, DR5 was expressed in ATLL-related cell lines[28] but tumor necrosis factor-R1 mostly was not (not shown) and there was no change after LBH589 treatment (not shown). LBH589 rather reduced Fas expression in ST1, LMY1 and HuT102 cells (Figure 4a). In typical DR-mediated apoptosis (Jurkat + TRAIL), both extrinsic and intrinsic pathways are activated including cleavage of BID, which was not observed in K562 cells treated with 12 nM of LBH589 (Figure 4c). In ATLL cell lines, western blotting revealed no bands of cleaved caspase-8 on treatment with LBH589 (Figure 4b). This was accompanied by slight changes in FADD and BID expression (Figure 4b). In contrast, LBH589 reduced the expression of FLIP proteins in HuT102 and KK1 cells (Figure 4b). Fluorometric analysis eventually showed that LBH589 little

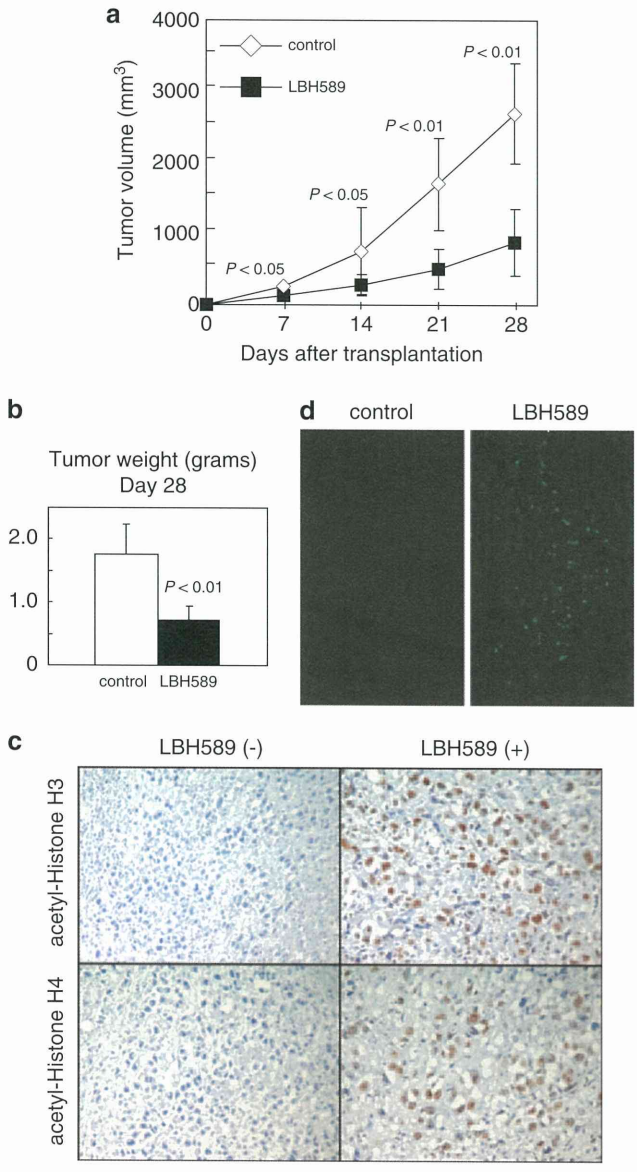

Figure 3 LBH589 reduces tumors inoculated in SCID mice. HuT102 cells (10^7 per mouse) were injected subcutaneously into SCID mice. The mice (five per group) were treated with either vehicle or LBH589. Treatment was initiated on the day after inoculation. Tumor volume and weight were monitored on the indicated days after the injection of cells. (**a**) Serial changes in tumor volume in treated and untreated mice. Data are the mean ± s.d. for five mice each. Mann–Whitney's *U*-test was used to compare results with control values. (**b**) Tumors removed from untreated mice and LBH589-treated mice on day 28 after cell inoculation were weighed. (**c**) Immunohistochemical staining shows the acetylation of histones H3/H4 in tumors of treated mice. (**d**) TUNEL assays show apoptotic cells in tumors from mice treated with LBH589 compared with the control mice. Magnification, ×40.

activated caspase-8 in ATLL-related cell lines in contrast to caspase-9 (Figure 4d). These results suggest that LBH589 does not activate the extrinsic pathway in ATLL-related cell lines.

LBH589 induces apoptosis in ATLL cells by activating the intrinsic pathway

Next, we investigated the changes in permeability of the mitochondrial membrane in cells treated with LBH589 by using the 5, 5′, 6, 6′-tetrachloro-1, 1′, 3, 3′-tetraethylbenzimidazolcarbocyanine iodide dye. The percentage of cells with decreased red fluorescence was increased from 7.3 to 81% and from 11 to 76% in ST1 and HuT102 cells, respectively (Figure 4e). Time course analyses of these changes are shown in Figure 4f. Furthermore, the release of cytochrome-*c* from mitochondria to the cytosol was detected by western blotting (Figure 4g). The activation of caspase-9 was confirmed by the appearance of cleaved caspase-9 and by a fluorometric analysis, which showed a three–eightfold increase after treatment with LBH589 (Figures 4b and d). The bands of cleaved caspase-3 and cleaved PARP, as a result of apoptosis, were clearly observed (Figure 4b). Collectively, these results suggest that the major mechanism of LBH589-induced apoptosis is activation of the intrinsic pathway.

Contribution of caspase-9 and/or AKT in LBH589-induced apoptosis

Interestingly, the band for pro-caspase-9 did not decrease in intensity in spite of its consumption but rather increased on treatment with LBH589 (Figure 4b). AKT has been shown to downregulate the expression of caspase-9 via direct phosphorylation[36] and LBH589 significantly reduced the expression of phospho-AKT (Figure 1c). Then, we used a typical PI3K/AKT inhibitor, LY294002, to investigate the impact of AKT's inactivation in LBH-induced apoptosis. ATLL cell lines with phospho-AKT actually underwent apoptosis and showed a decrease in phospho-AKT on treatment with LY294002. In this setting, however, the expression of caspase-9 was not upregulated (not shown). Furthermore, we performed transfection experiments with myr-AKT. The expression levels of phospho-AKT were not decreased by LBH589 in myr-AKT-transfected HuT102 cells (Supplementary Figure 1B). In this setting, we found that the percentage of Annexin-V-positive cells was decreased in myr-AKT cells (Supplementary Figure 1A). Expression levels of cleaved caspase-3 in LBH589-treated myr-AKT cells were moderately lower than those in mock-transfected cells (Supplementary Figure 1B). However, expression levels of other key molecules including caspase-9 were not altered (Supplementary Figure 1B). These results suggest that the LBH589-induced decrease in phospho-Akt levels is not an event upstream of the LBH589-induced accumulation of caspase-9 but partly contributes to the pro-apoptotic effects of LBH589.

Microarray analysis

We performed a DNA microarray analysis using HuT102 and LM-Y1 cells and compared gene expression profiles between cells treated with LBH589 and cells left untreated focusing on how the intrinsic pathway is activated during LBH589-induced apoptosis (Table 1). Among commonly observed changes, an upregulation of cytochrome-*c* expression and a downregulation of p53 expression were remarkable. An upregulation of caspase-9 expression and a downregulation of FAS expression, were in accord with results of western blotting and flow cytometric analysis, respectively (Figures 4a and b). Taking into consideration the results of the microarray analysis, we performed further studies focusing on three different groups; ATLL-characteristic, p53-related and caspase-2-related proteins.

Analysis of proteins characteristic of ATLL cells

We first focused on CCR4 and IL-2R, which were remarkably affected by LBH589 (Table 1). A majority of ATLL cells

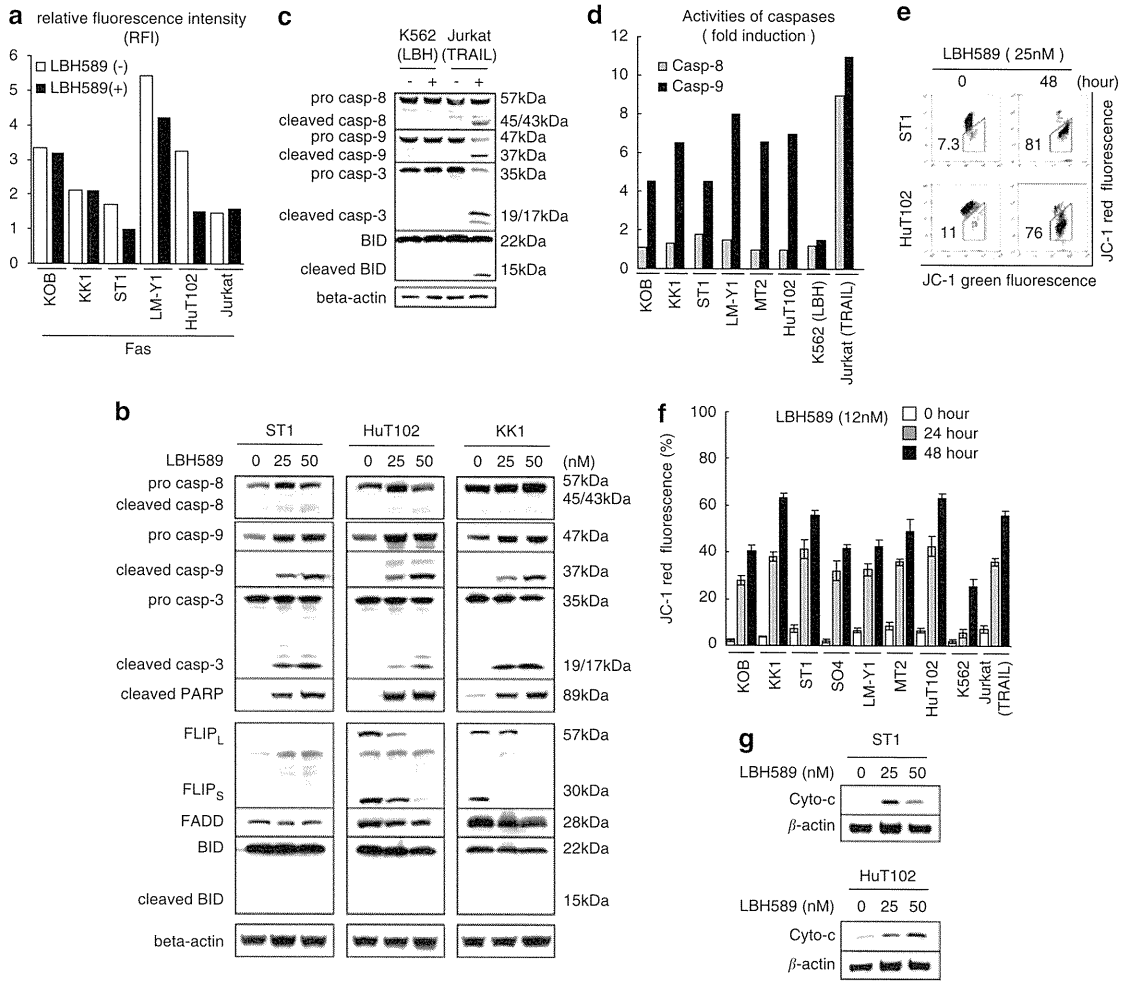

Figure 4 Analysis of the apoptotic pathway in LBH589-induced cell death. Cells were treated with either vehicle or the indicated concentrations of LBH589 for 24–48 h. After cells were harvested, flow cytometric analysis (FCM) (**a**, **d**, **e** and **f**) or western blotting (**b** and **g**) was performed. Tumor necrosis factor-related apoptosis-inducing ligand (TRAIL) (100 ng/ml)-treated Jurkat cells were used as a positive control of typical apoptosis and LBH589 (12 nM)-treated K562 cells were used as a negative control (**c**, **d** and **f**). (**a**) Changes in expression of Fas were indicated using RFI (the ratio of mean fluorescence intensity for specific staining to that for control staining). (**d**) Activities of caspases. Cells were incubated with the IETD-FMK for caspase-8, conjugated to FITC (FITC-IETD-FMK) or the LEHD-FMK for caspase-9, conjugated to FITC (FITC-LEHD-FMK) and analyzed using FCM. Comparison of the fluorescence intensity in the treated sample with that of the untreated control allows determination of the fold increase in activity of each caspase. (**e** and **f**) Mitochondrial membrane permeability. Cells were incubated with the JC-1 dye and analyzed using FCM. The percentage of cells with low JC-1 red fluorescence was evaluated. (**b**, **c** and **g**) Western blotting was performed using whole-cell lysate (**b** and **c**) or a cytosolic fraction (**g**) prepared as described in Materials and methods.

consistently express CCR4, which contributes to tumor cell progression and/or invasion.[37] ATLL-related cell lines had high levels of CCR4, which were dramatically decreased by LBH589 treatment (Figure 5a). IL-2R is also known to be overexpressed in ATLL cells and is often used as a diagnostic marker for ATLL.[17] LBH589 repressed the expression of IL-2R ~50% in the ATLL-related cell lines though levels were still extremely high (Figure 5b). Importantly, IL-2R is a typical gene whose promoter is activated by HTLV-1 Tax. Then, we investigated whether the expression of Tax mRNA is also affected by LBH589. The effect depended on the cells examined. In cells with high Tax mRNA levels (KOB, MT2 and HuT102), the expression tended to increase with LBH589 treatment, while in cells with relatively low Tax mRNA levels (LMY1, KK1 ST1 and SO4), it tended to decrease (Figure 5c). These results were consistent with those of western blotting (Figure 5c upper panel). The behavior of the HBZ mRNA was similar to that of the Tax mRNA; cells with high Tax levels tended to show an increase in HBZ mRNA on LBH589 treatment, while cells with lower Tax levels tended to exhibit a decrease (Figure 5d). In contrast, LBH589 significantly repressed HBZ-SI mRNA expression in ATLL-related cell lines except MT2 cells (Figure 5e). Protein levels of HBZ and HBZ-SI were not high in any cells examined and the expression profiles were approximately the same as those for the mRNA (Figures 5d and e). As NF-κB is constitutively activated in ATLL cells dependent on and/or independent of HTLV-1 Tax[38,39] and the repression of NF-κB is an important mechanism in DACi-induced ATLL cell death,[40,41] we examined the activities of NF-κB. However, repression of NF-κB by LBH589 was not commonly observed in ATLL-related cell lines (not shown).

LBH589-induced apoptosis in ATLL cells does not depend on the p53 pathway

Although p53 is an important inducer of the intrinsic apoptotic pathway, its gene expression was significantly decreased by LBH589 treatment (Table 1). To verify this phenomenon, we performed a luciferase assay with pG13-Luc using ST1, HuT102, KOB and KK1 cells and found that activation of p53 had not occurred (not shown). Unexpectedly, LBH589 reduced the

Table 1 Microarray analysis of HuT102 cells

Symbol	*Gene*	*Fold change*	
		HuT102	*LM-Y1*
SPP1	Secreted phosphoprotein 1 (osteopontin, bone sialoprotein I, early T-lymphocyte activation-1)	6.4	9.4
DHRS2	Dehydrogenase/reductase (SDR family) member-2	6.2	2.5
SERPINB2	Serpin peptidase inhibitor, clade B (ovalbumin), member-2	5.6	3.8
CASP9	Caspase 9, apoptosis-related cysteine peptidase	3.9	1.7
BTG2	BTG family, member-2	3.4	2.2
CYCS	Cytochrome-c, somatic	3.4	2.1
CLU	Clusterin	3.1	2.1
CTSB	Cathepsin B	3.1	3.5
GADD45B	Growth arrest and DNA damage inducible, beta	2.9	3.6
PHLDA1	Pleckstrin homology-like domain, family A, member-1	2.9	2.0
EFHC1	EF-hand domain (C-terminal) containing 1	2.8	2.6
IFI6	Interferon, alpha-inducible protein 6	2.7	2.2
NLRP1	NLR family, pyrin domain containing 1	2.7	1.1
LOH11CR2A	Loss of heterozygosity, 11, chromosomal region 2, gene A	2.6	2.3
RARRES3	Retinoic acid receptor responder (tazarotene induced) 3	2.5	2.5
ARHGAP20	Rho GTPase activating protein 20	2.3	1.7
BCL10	B-cell CLL/lymphoma 10	2.3	1.5
BTG1	B-cell translocation gene 1, anti-proliferative	2.3	1.4
ACVR1C	Activin A receptor, type IC	2.2	1.0
FASLG	Fas ligand (TNF superfamily, member-6)	2.2	—
RECK	Reversion-inducing-cysteine-rich protein with kazal motifs	2.2	—
SIAH2	Seven in absentia homolog 2 (*Drosophia*)	2.2	—
APAF1	Apoptotic peptidase-activating factor-1	2.1	1.5
ATM	Ataxia telangiectasia mutated (includes complementation groups A, C and D)	2.1	—
CRADD	CASP2 and RIPK1 domain containing adaptor with death domain	2.1	1.6
RIPK1	Receptor (TNFRSF)-interacting serine-threonine kinase-1	2.1	1.3
LTA	Lymphotoxin alpha (TNF superfamily, member-1)	−6.1	—
IL10	Interleukin-10	−4.4	—
TNFRSF8	Tumor necrosis factor receptor superfamily, member-8	−4.2	—
CCR4	Chemokine (C-C motif) receptor 4	−3.8	−2.6
IL2RA	Interleukin-2 receptor, alpha	−3.8	−2.6
TP53	Tumor protein p53 (Li-Fraumeni syndrome)	−3.5	−1.5
IKZF1	IKAROS family zinc finger-1 (Ikaros)	−3.4	−2.1
CCNB1	Cyclin B1	−3.3	−3.8
FAS	Fas (TNF receptor superfamily, member-6)	−3.3	−1.6
MKI67	Antigen identified by monoclonal antibody Ki-67	−3.2	−4.4
CDC2	Cell division cycle 2, G1 to S and G2 to M	−3.2	—
PLK1	Polo-like kinase 1 (Drosophila)	−3.0	−1.4
SULF1	Sulfatase 1	−3.0	—
BIRC5	Baculoviral IAP repeat-containing 5 (survivin)	−2.9	−3.8
CDK2AP1	CDK2-associated protein-1	−2.9	−1.1
AVEN	Apoptosis, caspase activation inhibitor	−2.8	—
MCM5	Minichromosome maintenance complex component-5	−2.8	−3.5
CDC25A	Cell division cycle 25 homolog A (*Schizosaccharomyces pombe*)	−2.7	−4.0
MYBL2	v-myb Myeloblastosis viral oncogene homolog (avian)-like-2	−2.7	−4.0
MYC	v-myc Myelocytomatosis viral oncogene homolog (avian)	−2.7	−1.9
BUB1B	BUB1 budding uninhibited by benzimidazoles 1 homolog beta (yeast)	−2.6	−4.1
CDCA3	Cell division cycle associated-3	−2.6	−3.5
FAIM	Fas apoptotic inhibitory molecule	−2.6	−2.1
ATF5	Activating transcription factor-5	−2.5	−3.3
WEE1	WEE1 homolog (*Schizosaccharomyces pombe*)	−2.5	−2.8
BCAT1	Branched chain aminotransferase 1, cytosolic	−2.4	−2.1
CCNA2	Cyclin A2	−2.4	−3.8
STEAP3	STEAP family member 3	−2.4	−1.3
ZAK	Sterile alpha motif and leucine zipper containing kinase AZK	−2.4	−3.2
CCNB2	Cyclin B2	−2.3	−3.8
FBXO5	F-box protein-5	−2.3	−2.6
HMGB1	High-mobility group box 1	−2.3	−2.7
NEK6	NIMA (never in mitosis gene a)-related kinase-6	−2.3	−3.2
RYR1	Ryanodine receptor 1 (skeletal)	−2.3	—
SFRS2	Splicing factor, arginine/serine-rich-2	−2.3	−1.7
AURKA	Aurora kinase A	−2.2	−3.0
BCLAF1	BCL2-associated transcription factor 1	−2.2	−1.9
CXCR4	Chemokine (C-X-C motif) receptor-4	−2.2	−1.7
E2F8	E2F transcription factor-8	−2.2	−3.4
CDC45L	CDC45 cell division cycle 45-like (S. cerevisiae)	−2.1	−4.3
CSE1L	CSE1 chromosome segregation 1-like (yeast)	−2.1	−1.8
HK2	Hexokinase-2	−2.1	—
NME1	Non-metastatic cells 1, protein (NM23A) expressed in	−2.1	−1.3

Abbreviation: TNF, tumor necrosis factor. HuT102 and LM-Y1 cells were treated with either vehicle or 50 nM of LBH589 for 24 h and DNA microarray analyses were performed. Among genes with changes in expression of at least 2.1-fold (log 2 ratio) in either direction in HuT102 cells, we picked those with known functions related to apoptosis, the cell cycle and cell proliferation.

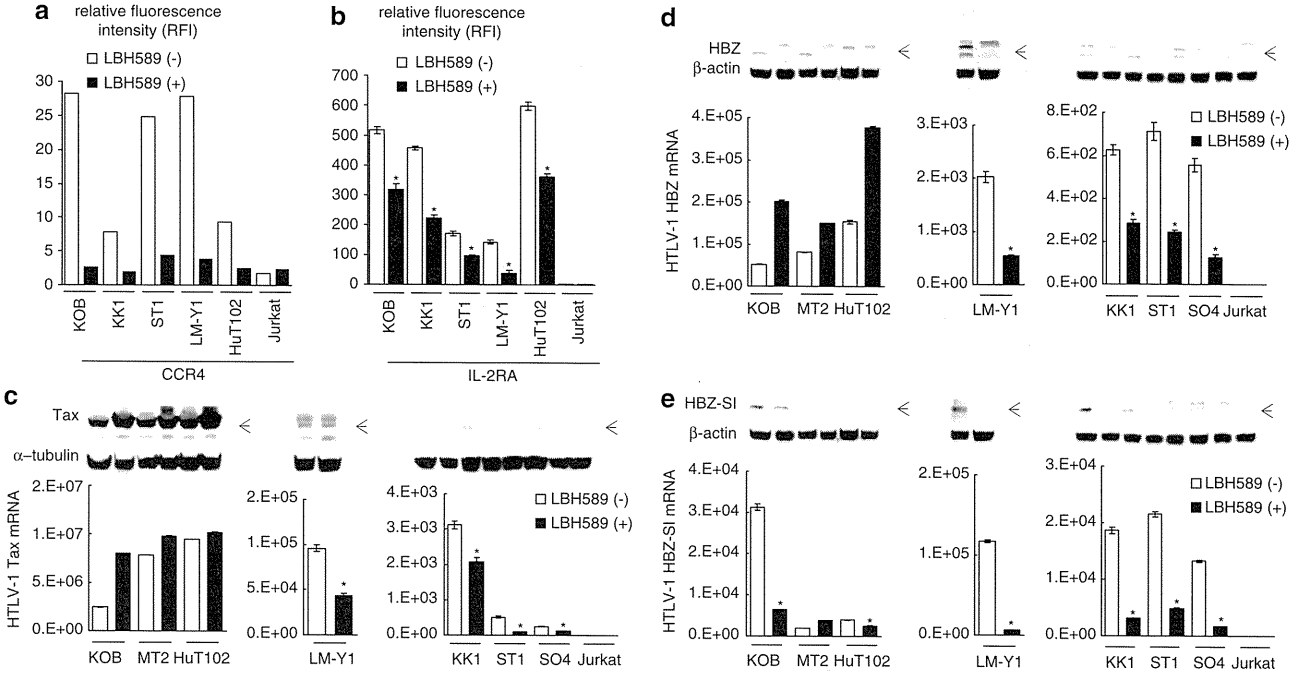

Figure 5 Effect of LBH589 on proteins characteristic of adult T-cell leukemia/lymphoma (ATLL) cells. Cells were treated with either vehicle or 50 nM of LBH589 for 24 h. After cells were harvested, flow cytometric analysis (FCM), real time quantitative RT-PCR and western blotting were performed. (**a** and **b**) Changes in expression of CCR4 and IL-2R were evaluated by FCM. The results were indicated using RFI. (**c**–**e**) Real-time quantitative RT-PCR and western blotting against HTLV-1 Tax, HBZ and HBZ-SI were performed as described in materials and methods. RT-PCRs were carried out in duplicate and the average value was used as the absolute amount of each mRNA. The cells were divided into three groups according to the amount of Tax mRNA; cell lines with high Tax mRNA levels (KOB, MT2 and HuT102), moderate levels (LM-Y1) and low levels (KK1 ST1 and SO4). The results of western blotting are also shown in each panel. (**b**–**e**) Results were expressed as the mean ± s.d. for three independent experiments and were also analyzed using Student's *t*-test. $^*P<0.01$.

expression of p53 in ST1 and KK1 as well as HuT102 cells without any accumulation of MDM2, which degrades p53 (Figure 6a). In contrast, the band of p21 was increased in intensity in these cell lines irrespective of their p53 status. Among apoptosis-related proteins downstream of p53, we found an increase in survivin, a decrease in XIAP, and no change in BAX, PUMA and Bcl-2 on treatment with LBH589 in ST1 or HuT102 cells. These results suggest that typical Bcl-2 family members are not involved in the permeabilization of the mitochondrial membrane in LBH589-induced apoptosis. Interestingly, LBH589 increased the expression of Bax and PUMA and decreased that of Bcl-2 and Bcl-xL in KK1 cells carrying a non-functional p53 mutation. These results indicate that LBH589 induced apoptosis in ATLL-related cell lines in a p53-independent manner.

Analysis of caspase-2-related apoptotic pathway

CASP2 and RIPK1 domain containing adaptor with death domain (also known as RAIDD), RIP, caspase-9 and cytochrome-*c* are involved in caspase-2-mediated apoptosis and were upregulated in their expression after LBH589 treatment (Table 1). The apoptosis induced by tumor necrosis factor-R1 requires the adaptor proteins TRADD, RIP and RAIDD in addition to caspase-2.[42] Recent reports suggest that caspase-2 can cause cytochrome-*c*'s release from mitochondria directly or indirectly.[43,44] Additionally, PIDD can interact with RAIDD and caspase-2, forming a PIDDosome and inducing apoptosis.[45] We investigated the expression profiles of caspase-2-related proteins by western blotting (Figures 6b and c). Caspase-2 was clearly activated by the treatment with LBH589 and cleaved forms were observed. Similar results were observed in TRAIL-treated Jurkat cells (Figure 6c). PIDD (90kDa) is constitutively processed into 51 and 37 kDa forms and cleaved PIDD (37 kDa) is essential for the activation of caspase-2.[46] Furthermore, upregulation of the expression of general forms of PIDD was observed during the activation of caspase-2 induced by genotoxic agents.[46] ATLL cell lines and Jurkat cells expressed various forms of PIDD, levels of which were not increased by LBH589 or TRAIL (Figures 6b and c). RIP was increased and TRADD was decreased in KK1 cells but neither was changed in ST1 or HuT102 cells. Of note, the activation of RAIDD was a common characteristic in these cells. Furthermore, the activation of RAIDD was also observed at the mRNA level in most of the ATLL-related cell lines (Figure 6d). In KK1 and ST1 cells, the activation of RAIDD mRNA expression was faint whereas that of protein production was obvious. We analyzed the 20s proteasome's activities to investigate whether RAIDD regulation by LBH589 in these cells is due to proteasome inhibition (Supplementary Figure 1C). Activities of 20S proteasome were dramatically impaired by MG132 in all cells examined and were not changed by LBH589 in KK1 and ST1 cells. The expression of RAIDD mRNA was not induced by the various chemicals used except LBH589 (Figure 6d, Supplementary Figure 1C, and data not shown). These results suggest that LBH589 caused the activation of caspase-2 and RAIDD without activating p53 and PIDD. We further observed the activation of RAIDD and caspase-2 in addition to acetylated histones in primary ATLL cells (Figure 6e).

LBH589 induces apoptosis in ATLL cells via caspase-2's activation

To further investigate the role of caspase-2-mediated apoptosis in LBH589-induced cell death, we first performed inhibition

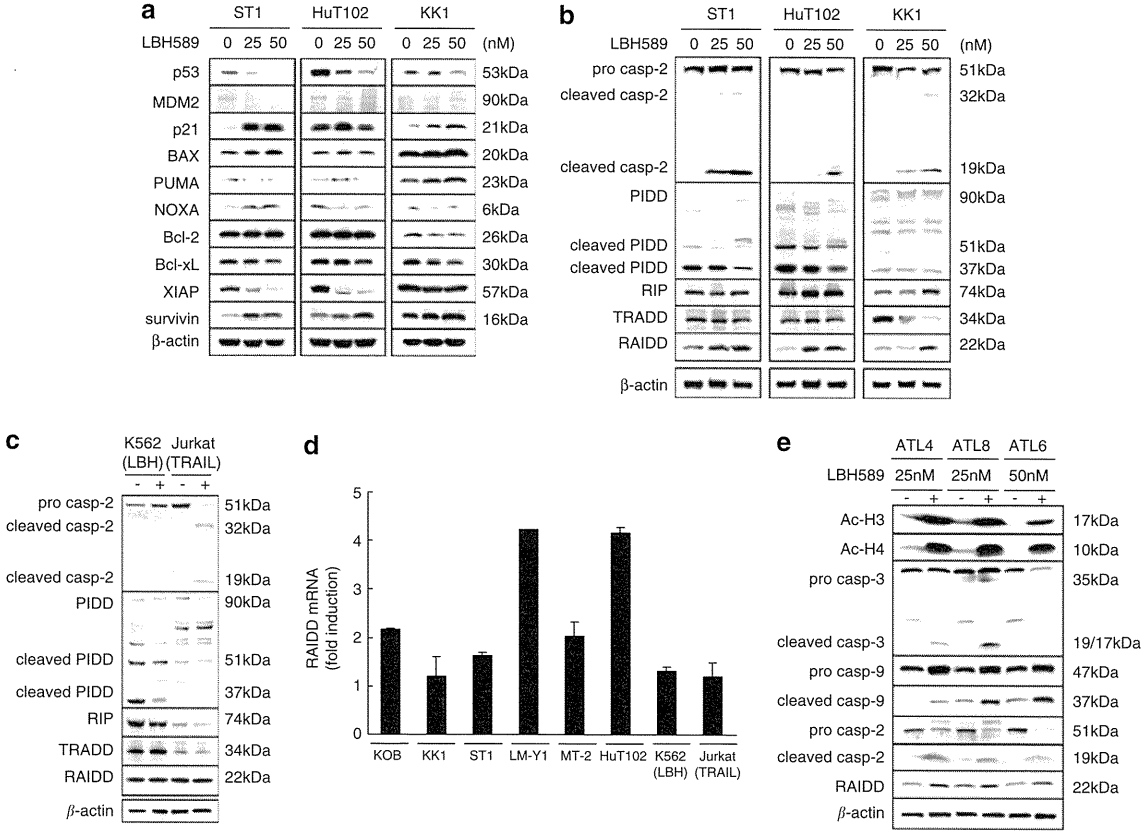

Figure 6 LBH589 activates RAIDD and caspase-2, but not p53. Whether the p53 pathway or caspase-2-related factors contribute to the LBH589-induced cell death was investigated by using ST1 and HuT102 (p53 wild type) cells, and KK1 (p53 mutated) cells. (**a**, **b** and **e**) Cells were treated with either vehicle or the indicated concentrations of LBH589 for 24 h. After cells were harvested, western blotting was performed. (**c**) Western blotting: tumor necrosis factor-related apoptosis-inducing ligand (TRAIL) (100 ng/ml)-treated Jurkat cells were used as a positive control of typical apoptosis and LBH589 (12 nM)-treated K562 cells were used as a negative control. (**d**) Activation of RAIDD by LBH589. After cells were treated with either vehicle or 50 nM of LBH589 for 24 h, real-time quantitative RT-PCR for RAIDD was performed. The fold increase in each cell line was obtained by setting the value for the expression without LBH589 as 1.0.

assays of caspases using specific inhibitors. The proportion of Annexin-V-positive cells among TRAIL-treated Jurkat cells was reduced from 67 to 20% by the pan-caspase inhibitor Z-VAD (Figure 7a). LBH589-induced cell death was also attenuated by Z-VAD with the percentage of Annexin-V-positive cells decreasing from 47 and 54% to 16 and 21% in ST1 and HuT102 cells, respectively. The caspase-8 inhibitor was not effective against LBH589-induced cell death, consistent with the finding that caspase-8 was not activated (Figure 4d). Importantly, the caspase-2 inhibitor Z-VDVAD had a similar effect to Z-VAD in LBH589-treated Jurkat cells, while it had a weak effect in TRAIL-treated cells (46%). Furthermore, western blotting revealed that the cleavage of caspase-3 by LBH589 was inhibited by Z-VDVAD as well as Z-VAD (not shown). These results suggest that LBH589 causes apoptosis in ATLL-related cell lines in a caspase-dependent manner and activation of caspase-2 is essential.

RAIDD as well as caspase-2 has a critical role in LBH589-induced apoptosis

Next, we performed siRNA experiments targeting caspase-2, caspase-9, RAIDD, PIDD and RIP to disclose the key triggers of apoptosis. Annexin-V/PI assays revealed that siRNA of RAIDD significantly repressed LBH-induced cell death, as did si-caspase-2 (Figure 7b). The proportion of Annexin-V-positive cells was ~65% in si-control cells and 37% in ST1 si-RAIDD cells. Similar results were obtained with HuT102 cells using siRNA set #1 (Figure 7b), set #2, and set #3 (Supplementary Figure 2C and E). Si-caspase-9 also inhibited LBH589-induced cell death while si-PIDD and si-RIP caused no change (Figure 7b). Similar inhibitory effects by si-RAIDD and si-caspase-2 were observed in JC-1 experiments (Figure 7c). The effect of si-caspase-9 was less extensive than that of si-PIDD or si-RIP (Figure 7c). These results suggest that RAIDD as well as caspase-2 has a critical role in LBH589-induced apoptosis and, importantly, they have active roles upstream of the mitochondria.

RAIDD has an initiating role in LBH589-induced apoptosis

Western blotting revealed that si-caspase-2 suppressed the cleavage of caspase-9, caspase-3 and PARP as well as the expression of caspase-2 itself. However, it could not suppress the activation of RAIDD (Figure 7d). Si-caspase-9 suppressed the cleavage of caspase-3 and PARP as well as the expression of caspase-9 itself, but could not suppress the activation of caspase-2 or RAIDD. Of note, si-RAIDD most effectively suppressed the cleavage of caspase-2, caspase-9, caspase-3 and PARP as well as the upregulation of RAIDD expression. Si-PIDD and si-RIP did not alter the expression profiles of caspases and RAIDD. These changes were basically similar in ST1 and HuT102 cells. An additional siRNA experiment was

performed using set #2 and set #3 siRNAs and results were similar to Figure 7d (Supplementary Figure 2D and F). The results indicate that the activation of RAIDD occurs upstream of the activation of caspase-2 and has an initiating role in LBH589-induced apoptosis.

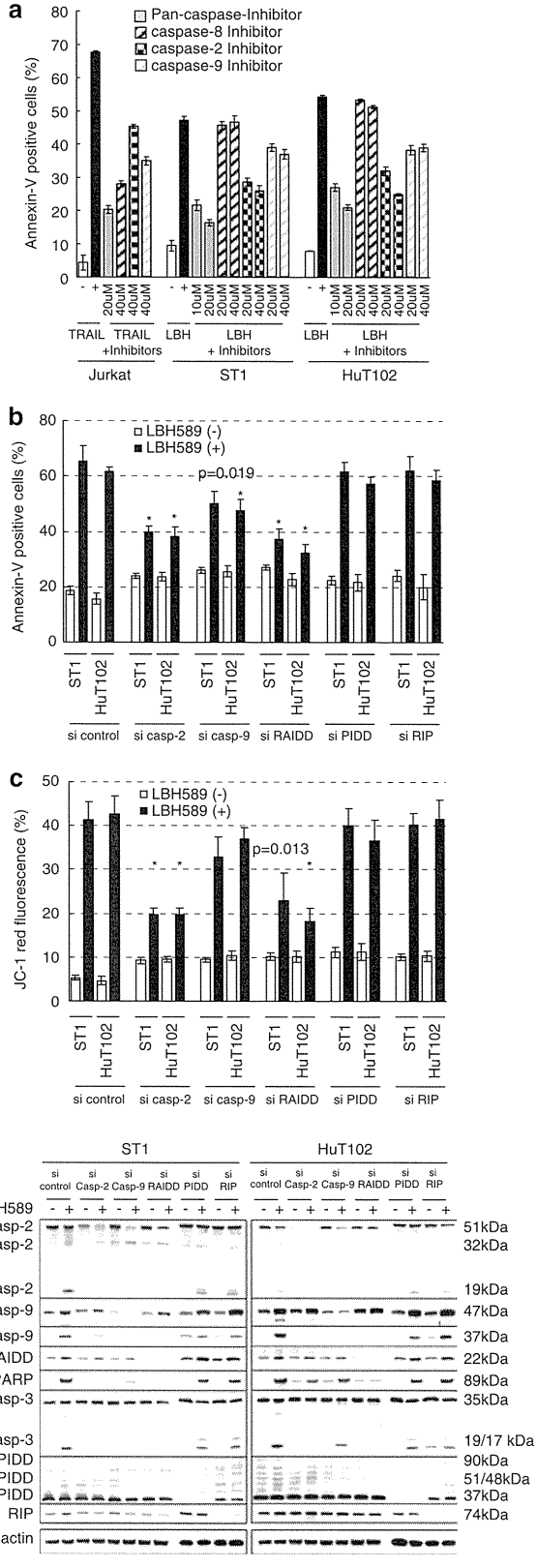

Discussion

DACi achieved significant biological effects in preclinical models of cancer including hematological malignancies which has led to clinical trials.[4,47–49] Then, it has become important to re-evaluate the mechanisms of tumor cell death caused by DACi. These processes will improve the design of further clinical trials and help in developing novel DACi. In this study, we showed that a newly developed DACi, LBH589, effectively induces ATLL cell death both *in vitro* and *in vivo* by a unique mechanism that has not been reported. Our findings uncovered a new role of caspase-2's activation in the induction of apoptosis.

It has been recognized that caspase-2-mediated apoptosis is initiated by death receptors.[42,50] However, recent studies revealed the ability of caspase-2 to engage the intrinsic pathway in response to DNA damage.[43,51–53] One possibility is that caspase-2 acts indirectly on the mitochondria, by cleaving the pro-apoptotic protein BID or by activating Bax and inducing the release of cytochrome-*C*.[44] Another alternative is that caspase-2 directly permeabilizes the mitochondrial membrane and stimulates the release of cytochrome-*C* independently of the Bcl-2 family including Bax and Bcl-2.[54] In addition, a recent report indicated that caspase-2 became activated in the so called PIDDosome, a complex of PIDD, caspase-2 and RAIDD, in a p53-dependent manner.[45] In our study, si-caspase-2 and si-RAIDD inhibited LBH589-induced apoptosis as well as permeabilization of the mitochondrial membrane. This mechanism is similar to the PIDDosome, however, LBH589-induced apoptosis was independent of p53 and PIDD was not activated. In addition, si-PIDD or si-RIP did not alter LBH589-induced apoptosis. Si-caspase-2 could not suppress the activation of RAIDD while si-RAIDD effectively suppressed the cleavage of caspase-2. These results indicated that LBH589 caused the activation of caspase-2 followed by RAIDD independent of p53 and PIDD. Regarding this point, a previous report suggested that caspase-2's activation occurred in a p53-independent manner.[55] Furthermore, two recent studies using PIDD-deficient mice demonstrated the PIDDosome-independent activation of caspase-2.[56,57] From our results, si-caspase-2 attenuated the LBH589-induced permeabilization of the mitochondrial membrane and the mRNA expression of cytochrome-*C* was highly upregulated by LBH589 probably due to cytochrome-*C*'s release. In contrast, most of the Bcl-2 family proteins were not altered by LBH589. In this regard, Robertson *et al.* suggested that caspase-2 can directly stimulate the intrinsic pathway independent of the Bcl-2 family.[43] More recently, Sidi *et al.*

Figure 7 RAIDD has a critical role in initiating LBH589-induced apoptosis. (**a**) Inhibition assay of caspases. Cells were treated with 25 nM of LBH589 or 100 ng/ml of tumor necrosis factor-related apoptosis-inducing ligand (TRAIL) with indicated concentrations of caspase-inhibitors for 24 h. Results were evaluated by Annexin-V/PI staining. Experiments were performed in triplicate and results were expressed as the mean ± s.d. (**b** and **c**) Effects of siRNA against caspase-2, caspase-9, RAIDD, PIDD and RIP. At 24 h after transfection, cells were incubated for 24 h with either vehicle or 50 nM of LBH589. Results were evaluated using Annexin-V/PI staining or the JC-1 dye and analyzed with flow cytometric analysis. Results were expressed as the mean ± s.d. for three independent experiments and were also analyzed using Student's *t*-test. $*P<0.01$ compared with si-control. (**d**) Western blotting. At 24 h after transfection, cells were incubated for 24 h with either vehicle or 50 nM of LBH589 and western blotting was performed.

demonstrated a caspase-2-dependent apoptotic program that bypasses a deficiency of p53 and excess of Bcl-2.[58] These reports are partly consistent with our own observations. However, our scenario does not work without the activation of RAIDD. Therefore, our results suggest that ATLL cells make use of a unique RAIDD-caspase-2-induced intrinsic pathway, which has not been reported previously. Additionally, as caspase-2-mediated apoptosis requires caspase-9,[51] upregulation of caspase-9 expression by LBH589 is advantageous to the induction of apoptosis. Although a number of independent studies strongly support a role for the intrinsic pathway in DACi-induced apoptosis, the mechanism remains to be fully elucidated.[1] Our findings may provide some explanation.

Although there is a consensus that the p53 pathway is inactivated by Tax in ATLL cells,[59] we recently found that ATLL-related cell lines expressing the wild-type p53 harbor an intact p53 pathway.[31] Some previous findings highlighted the importance of p53 in the effect of DACi, however, other studies demonstrated that the expression of wild-type p53 is not necessary for DACi-induced apoptosis.[2,60,61] Meanwhile, it has been reported that p21, downstream of p53, is activated by DACi independent of p53.[62,63] Indeed, the expression of p21 was increased by LBH589 in ATLL-related cell lines irrespective of their p53 status. In the present study, we clearly showed that LBH589 does not activate p53 in ATLL-related cell lines with the wild-type p53, and LBH589 was also effective against p53-mutant cells via the induction of a p53-like pro-apoptotic response. A similar phenomenon was reported previously in that the DACi FR901228 caused a p53-like pro-apoptotic response in p53 mutant cells and the degradation of the mutant p53 protein.[64] We further confirmed that LBH589 caused the degradation of p53 protein in p53 wild-type cells as well as p53-mutant cells. These results suggest that some types of DACi including LBH589 act upstream of the p53 pathway and cause the degradation of even mutated p53 protein via an unknown mechanism.

We also explored the ATLL-specific mechanisms in LBH589-induced cell death. Notably, CCR4 and IL-2R, well-known molecular targets in ATLL therapy, were repressed by the LBH589 treatment.[65,66] We speculated that Tax participates in the suppression of IL-2R, however, cells with high Tax mRNA levels actually showed an increase in Tax mRNA expression after LBH589 treatment. These results indicate that LBH589 can cause apoptosis even in Tax-expressing ATLL cells. In our study, mRNA levels of Tax and HBZ in ATLL-related cell lines were not inversely correlated. In addition, after treatment with LBH589, mRNA levels of Tax and HBZ changed in parallel. These results are not consistent with the idea that HBZ can inhibit Tax's activation.[19] Meanwhile, the expression of HBZ-SI was suppressed by LBH589 in most of the ATLL-related cell lines. Although the precise function of HBZ-SI is still under investigation,[24] a previous study found that inhibition of HBZ-SI by shRNA resulted in cell growth inhibition in ATLL cells.[23] Thus, HBZ-SI could potentially be a molecular target in ATLL therapy and the decrease in HBZ-SI caused by LBH589 treatment may also contribute to the apoptosis of ATLL cells. Consequently, we demonstrated that LBH589 is a promising drug against ATLL, and also identified a novel intrinsic pathway in LBH589-induced apoptosis.

Conflict of interest

The authors declare no conflict of interest.

Acknowledgements

We would like to express our gratitude to Dr Mesnard JM, Institut de Biologie, Laboratoire Centre d'étude d'agents Pathogènes et Biotechnologies pour la Santé Montpellier, France. Grant support note: This study was supported in part by a Grant-in-aid for Scientific Research (20590580) from the Japan Society for the Promotion of Science and a grant from Novartis.

References

1 Baylin SB, Ohm JE. Epigenetic gene silencing in cancer—a mechanism for early oncogenic pathway addiction? *Nat Rev Cancer* 2006; **2**: 107–116.
2 Bolden JE, Peart MJ, Johnstone RW. Anticancer activities of histone deacetylase inhibitors. *Nat Rev Drug Discov* 2006; **9**: 769–984.
3 Minucci S, Pelicci PG. Histone deacetylase inhibitors and the promise of epigenetic (and more) treatments for cancer. *Nat Rev Cancer* 2006; **1**: 38–51.
4 Xu WS, Parmigiani RB, Marks PA. Histone deacetylase inhibitors: molecular mechanisms of action. *Oncogene* 2007; **37**: 5541–5552.
5 Peart MJ, Tainton KM, Ruefli AA, Dear AE, Sedelies KA, O'Reilly LA *et al.* Novel mechanisms of apoptosis induced by histone deacetylase inhibitors. *Cancer Res* 2003; **63**: 4460–4471.
6 Henderson C, Mizzau M, Paroni G, Maestro R, Schneider C, Brancolini C. Role of caspases, Bid, and p53 in the apoptotic response triggered by histone deacetylase inhibitors trichostatin-A (TSA) and suberoylanilide hydroxamic acid (SAHA). *J Biol Chem* 2003; **14**: 12579–12589.
7 Mitsiades N, Mitsiades CS, Richardson PG, McMullan C, Poulaki V, Fanourakis G *et al.* Molecular sequelae of histone deacetylase inhibition in human malignant B cells. *Blood* 2003; **101**: 4055–4062.
8 Maiso P, Carvajal-Vergara X, Ocio EM, Lopez-Perez R, Mateo G, Gutierrez N *et al.* The histone deacetylase inhibitor LBH589 is a potent antimyeloma agent that overcomes drug resistance. *Cancer Res* 2006; **66**: 5781–5789.
9 Fulda S, Debatin KM. Extrinsic versus intrinsic apoptosis pathways in anticancer chemotherapy. *Oncogene* 2006; **25**: 4798–4811.
10 Bao Q, Shi Y. Apoptosome: a platform for the activation of initiator caspases. *Cell Death Differ* 2007; **14**: 56–65.
11 Nimmanapalli R, Fuino L, Bali P, Gasparetto M, Glozak M, Tao J *et al.* Histone deacetylase inhibitor LAQ824 both lowers expression and promotes proteasomal degradation of Bcr-Abl and induces apoptosis of imatinib mesylate-sensitive or -refractory chronic myelogenous leukemia-blast crisis cells. *Cancer Res* 2003; **63**: 5126–5135.
12 Bali P, Pranpat M, Bradner J, Balasis M, Fiskus W, Guo F *et al.* Inhibition of histone deacetylase 6 acetylates and disrupts the chaperone function of heat shock protein 90: a novel basis for antileukemia activity of histone deacetylase inhibitors. *J Biol Chem* 2005; **280**: 26729–26734.
13 Kovacs JJ, Murphy PJ, Gaillard S, Zhao X, Wu JT, Nicchitta CV *et al.* HDAC6 regulates Hsp90 acetylation and chaperone-dependent activation of glucocorticoid receptor. *Mol Cell* 2005; **18**: 601–607.
14 George P, Bali P, Annavarapu S, Scuto A, Fiskus W, Guo F *et al.* Combination of the histone deacetylase inhibitor LBH589 and the hsp90 inhibitor 17-AAG is highly active against human CML-BC cells and AML cells with activating mutation of FLT-3. *Blood* 2005; **105**: 1768–1776.
15 Fiskus W, Pranpat M, Bali P, Balasis M, Kumaraswamy S, Boyapalle S *et al.* Combined effects of novel tyrosine kinase inhibitor AMN107 and histone deacetylase inhibitor LBH589 against Bcr-Abl-expressing human leukemia cells. *Blood* 2006; **108**: 645–652.
16 Yamada Y, Tomonaga M. The current status of therapy for adult T-cell leukaemia-lymphoma in Japan. *Leuk Lymphoma* 2003; **44**: 611–618.
17 Yoshida M. Discovery of HTLV-1, the first human retrovirus, its unique regulatory mechanisms, and insights into pathogenesis. *Oncogene* 2005; **24**: 5931–5937.